Primordial black holes from inflation and quantum diffusion

Journal of Cosmology and Astroparticle Physics
An IOP and SISSA journal

Primordial black holes from inflation and quantum diffusion

M. Biagetti,[a] **G. Franciolini,**[b] **A. Kehagias**[c] **and A. Riotto**[b]

[a]Institute of Physics, Universiteit van Amsterdam,
Science Park, 1098XH Amsterdam, The Netherlands
[b]Department of Theoretical Physics and Center for Astroparticle Physics (CAP),
24 quai E. Ansermet, CH-1211 Geneva 4, Switzerland
[c]Physics Division, National Technical University of Athens,
15780 Zografou Campus, Athens, Greece

E-mail: m.biagetti@uva.nl, gabriele.franciolini@unige.ch,
kehagias@central.ntua.gr, antonio.riotto@unige.ch

Received April 23, 2018
Accepted July 2, 2018
Published July 16, 2018

Abstract. Primordial black holes as dark matter may be generated in single-field models of inflation thanks to the enhancement at small scales of the comoving curvature perturbation. This mechanism requires leaving the slow-roll phase to enter a non-attractor phase during which the inflaton travels across a plateau and its velocity drops down exponentially. We argue that quantum diffusion has a significant impact on the primordial black hole mass fraction making the classical standard prediction not trustable.

Keywords: inflation, physics of the early universe, primordial black holes

ArXiv ePrint: 1804.07124

JCAP07(2018)032

 https://doi.org/10.1088/1475-7516/2018/07/032

Contents

1 Introduction

The interest in the physics of Primordial Black Holes (PBHs) and the possibility that they form all (or a fraction) of the dark matter in the universe has risen up [1–10] again after the discovery of two $\sim 30 M_\odot$ black holes through the gravitational waves generated during their merging [11]. A standard mechanism to account for the generation of the PBHs is through the boost of the curvature perturbation $\mathcal{R}$ at small scales [12–14]. Such an enhancement can occur either within single-field models of inflation, see refs. [15–19] for some recent literature, or through some spectator field [20–23] which could be identified the Higgs of the Standard Model [24].

In order for this primordial mechanism to occur, one needs an enhancement of the power spectrum of the curvature perturbation from its $\sim 10^{-9}$ value at large scales to $\sim 10^{-2}$ on small scales. Subsequently, these large perturbations are communicated to radiation during the reheating process after inflation and they may give rise to PBHs upon horizon re-entry if they are sizeable enough. If we indicate by $\mathcal{P}_\mathcal{R}$ the comoving curvature power spectrum, a region of size the Hubble radius may collapse and form a PBH if the corresponding square root of the variance $\sigma_\mathcal{R}$ smoothed with a high-pass filter on the same length scale (comoving momenta larger than the inverse of the comoving Hubble) is larger than some critical value $\mathcal{R}_c$. Its exact value is sensitive to the equation of state upon horizon re-entry and it is about 0.086 for radiation [25]. However, larger values have been adopted in the literature [26–28]. We will later on use the common representative value $\mathcal{R}_c \simeq 1.3$.

Under the (strong) hypothesis that the curvature perturbation obeys a Gaussian statistics, the primordial mass fraction $\beta_{\rm prim}(M)$ of the universe occupied by PBHs formed at the

JCAP07(2018)032

time of formation reads

$$\beta_{\rm prim}(M) = \int_{\mathcal{R}_c}^{\infty} \frac{{\rm d}\mathcal{R}}{\sqrt{2\pi}\,\sigma_{\mathcal{R}}} e^{-\mathcal{R}^2/2\sigma_{\mathcal{R}}^2}. \tag{1.1}$$

It corresponds to a present dark matter abundance made of PBH of masses M given by (neglecting accretion) [28]

$$\left(\frac{\Omega_{\rm DM}(M)h^2}{0.12}\right) \simeq \left(\frac{\beta_{\rm prim}(M)}{7\cdot 10^{-9}}\right)\left(\frac{\gamma}{0.2}\right)^{1/2}\left(\frac{106.75}{g_*}\right)^{1/4}\left(\frac{M_\odot}{M}\right)^{1/2}, \tag{1.2}$$

where $\gamma < 1$ is a parameter accounting for the efficiency of the collapse and g_* is the effective number of degrees of freedom. Imposing PBHs to be the dark matter, values $\gamma < 1$ require larger values of $\beta_{\rm prim}$ and therefore to be conservative we impose $\gamma = 1$ [28]

$$\beta_{\rm prim}(M) \gtrsim 3\cdot 10^{-9}\left(\frac{M}{M_\odot}\right)^{1/2}. \tag{1.3}$$

For a mass of the order of $10^{-15}\,M_\odot$ we find [28]

$$\sigma_{\mathcal{R}} \gtrsim 0.16. \tag{1.4}$$

Now, in single-field models of inflation the power spectrum of the comoving curvature perturbation is given by (we set the Planckian mass equal to one from now on) [29]

$$\mathcal{P}_{\mathcal{R}}^{1/2}(k) = \left(\frac{H}{2\pi\phi'}\right), \quad \phi' = \frac{{\rm d}\phi}{{\rm d}N}, \tag{1.5}$$

where N is the number of e-folds, the prime denotes differentiation with respect to N, and H is the Hubble rate. The generation of PBHs requires the jumping within a few e-folds ΔN of the value of the power spectrum of about seven orders of magnitude from its value on CMB scales. Without even specifying the single-field model of inflation, one may conclude that there must be a violation of the slow-roll condition as ϕ' must change rapidly with time. This may happen when the inflaton field goes through a so-called non-attractor phase (dubbed also ultra-slow-roll) [30–39] in the scalar potential, thus producing a sizeable resonance in the power spectrum of the curvature perturbation.

When the inflaton experiences a plateau in its potential, since ϕ' must be extremely small, a short non-attractor period is achieved during which the equation of motion of the inflaton background ϕ reduces to

$$\phi'' + 3\phi' + \frac{V_{,\phi}}{H^2} \simeq \phi'' + 3\phi' = 0, \tag{1.6}$$

where $_{,\phi}$ denotes differentiation with respect to the inflaton field ϕ with potential $V(\phi)$. The comoving curvature perturbation increases, due to its decaying mode which in fact is growing, as

$$\phi' \sim e^{-3N} \ \text{ and } \ \mathcal{P}_{\mathcal{R}}^{1/2} \sim e^{3N}. \tag{1.7}$$

It is this exponential growth which helps obtaining large fluctuations in the curvature perturbation and the formation of PBHs upon horizon re-entry during the radiation phase. This is also the reason why the power spectrum should be quoted at the end of inflation and not, as usually done in slow-roll, at Hubble crossing: its value at the instant of Hubble crossing

JCAP07(2018)032

differs by a significant factor from the asymptotic value at late times. Not respecting these rules might lead to an incorrect estimate of the power spectrum and consequently of the PBH abundance at formation, see e.g. ref. [40] and the subsequent discussions in refs. [28, 36].

Putting aside the strong sensitivity of the PBH mass fraction at formation to possible non-Gaussianities [14, 41–50] which is common to all mechanisms giving rise to PBHs through sizeable perturbations (we will however devote appendix C for some considerations about non-Gaussianity where we will show that the δN formalism [51] can help in assessing the role of non-Gaussianity for those perturbations generated during the non-attractor phase) in this paper we are interested in another issue, the role of quantum diffusion. One might be reasonably suspicious that during the non-attractor phase the quantum diffusion becomes relevant [49]. The reason is the following. The stochastic equation of motion for the classical inflaton field takes into account that each Hubble time the inflaton field receives kicks of the order of $\pm(H/2\pi)$ [52]

$$\phi'' + 3\phi' + \frac{V_{,\phi}}{H^2} = \xi, \tag{1.8}$$

where ξ is a Gaussian random noise with

$$\langle \xi(N)\xi(N')\rangle = \frac{9H^2}{4\pi^2}\delta(N-N'). \tag{1.9}$$

During the non-attractor phase, $V_{,\phi}$ needs to be tiny enough to allow ϕ' to promptly decrease thus violating slow-roll. For the same reason, one needs to make sure that quantum jumps are not significant in this case. One could try to impose the condition

$$\frac{2\pi V_{,\phi}}{3H^3} \gtrsim 1. \tag{1.10}$$

to be satisfied during the non-attractor phase. In slow-roll, the condition (1.10) could be exactly expressed in terms of the power spectrum and the latter would be required to be smaller than unity, thereby giving a direct constraint on a physical observable. However, during the non-attractor phase, the bound (1.10) is not directly expressed in terms of the power spectrum (1.5), making the comparison with physical observables more difficult. One might naively think that during the non-attractor phase the noise is not relevant if ϕ' is larger than $(H/2\pi)$ [17]. However, this is not correct for two reasons. First because, as we will see, the relevant noise to be evaluated is the one for the inflaton velocity. Secondly, and above all, because this is not the right criterion to evaluate the strong impact of quantum diffusion onto the PBH mass fraction.

We will first elaborate on the computation of the power spectrum during the non-attractor phase in order to understand some basic features of the power spectrum itself, e.g. its time evolution and the location of its peak. This will be useful for the considerations about the quantum diffusion. We will then use the so-called Kramers-Moyal equation [53] to assess the impact of quantum diffusion.

The Kramers-Moyal equation is the suitable starting point as it highlights the importance of the inflaton velocity and it is a generalisation of the Fokker-Planck equation. Indeed, in general the Kramers-Moyal equation contains an infinite number of derivatives with respect to the inflaton field after having integrated out the velocity, while the Fokker-Planck equation is a truncation of the Kramers-Moyal equation by retaining only two spatial derivatives of the inflaton field. This is not an irrelevant point: Pawula's theorem [54] tells us that if we set to zero some coefficient c_n of the higher derivative terms with respect to the inflaton

JCAP07(2018)032

field with $n \geq 3$, then all the coefficients of the higher derivatives are zero. It is therefore not consistent to keep some higher derivative term unless all of them are kept. This means that, whenever the Kramers-Moyal equation may not be solved exactly, a numerical approach is useful to solve it without applying an unjustified truncation.

We will present both analytical and numerical results to quantify the impact of quantum diffusion on the PBH abundance. In the simplest case of non-attractor phase with an approximately linear or quadratic potential, the system can be solved analytically. For a linear potential, the stochastic motion of the system is characterised by the fact that the variance of the velocity ϕ' rapidly converges towards a stationary value. For a quadratic potential, the spread in the velocity varies with time, although slowly, away from the stationary point.

However, for more complicated situations, e.g. if during the non-attractor phase the inflaton goes through an inflection point, a numerical analysis is called for and we will show that the spread in the velocity grows with time. If this growth is too large, classicality as well as information on the PBH abundance is lost. We will propose two criteria to be respected in order to neglect the quantum diffusion and we will see that the curvature perturbation is severely constrained from above in order to avoid an undesirable spreading of the velocity wave packet. We will also argue that the capability of the standard (that is classical) calculation to predict the correct dark matter abundance in terms of PBH is severely challenged by the presence of quantum diffusion.

This paper is organised as follows. In section 2 we discuss the computation of the curvature perturbation during the non-attractor phase. We then start our study of the quantum diffusion, both analytically and numerically, in section 3 and 4 respectively. In sections 5 and 6 we offer two criteria to assess the importance of the diffusion. Finally, in section 7 we offer our conclusions.

The paper contains several appendices. Appendix A deals with the curvature perturbation, the Schwarzian derivative and the dual transformation; appendix B with the study of the evolution of the comoving curvature perturbation from the non-attractor phase back to the slow-roll phase; appendix C offers some consideration about non-Gaussianity.

2 The comoving curvature perturbation and the non-attractor phase

In this section we offer some considerations about the curvature perturbation generated thanks to the non-attractor phase. We start by some analytical considerations and then we will proceed with a more realistic example.

Non-attractor: some analytical considerations. We are interested in the curvature perturbation for those modes leaving the Hubble radius deep in the non-attractor phase. We suppose that the non-attractor phase starts when the inflaton field acquires the value ϕ_0 and ends when it becomes equal to $\phi_\star$. We also assume that the non-attractor phase is preceded and followed by slow-roll phases, see figure 1. During these phases $\eta = -\phi''/\phi'$ passes from a tiny value (slow-roll) to 3 (non-attractor) back to small values (slow-roll). To treat the problem analytically, we suppose that during the non-attractor phase we may Taylor expand the inflaton potential as

$$V(\phi) \simeq V_0 \left(1 + \sqrt{2\epsilon_V}(\phi - \phi_0)\right) + \cdots \quad \text{for} \quad \phi_\star < \phi < \phi_0, \tag{2.1}$$

where $\sqrt{2\epsilon_V} = V_{,\phi}/V_0$ is the slow-roll parameter. Of course, the potential during the non-attractor phase may be more complex, but its linearisation captures the main features.

JCAP07(2018)032

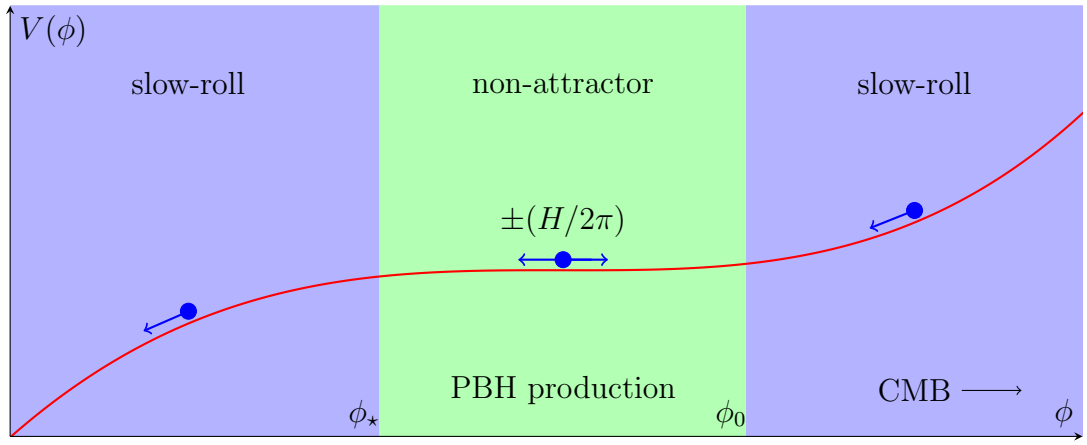

Figure 1. A representative behaviour of the inflaton potential during the various phases, highlighting the possibility of quantum diffusion during the non-attractor phase.

Computing everything in terms of the number of e-folds N and defining $N = 0$ the beginning of the non-attractor phase with initial conditions ϕ_0 and $\mathrm{d}\phi/\mathrm{d}N|_0 = \Pi_0$ and setting $\Pi(N) = \phi'(N)$, the solution of the equations of motion leads to

$$\begin{aligned}\phi(N) &= \phi_0 + \frac{1}{3}(\Pi_0 - \Pi) - \sqrt{2\epsilon_V}N,\\ \Pi(N) &= \sqrt{2\epsilon_V}\left(e^{-3N} - 1\right) + \Pi_0 e^{-3N}.\end{aligned} \tag{2.2}$$

We see that if the inflaton field starts with a large velocity from the preceeding slow-roll phase, there is a period over which the velocity of the inflaton field decays exponentially. Depending on the duration of the non-attractor phase, the velocity may or may not attain its slow-roll asymptote given by $-\sqrt{2\epsilon_V}$. Indicating by $\Pi_\star$ the value of the velocity at the end of the non-attractor phase, the final value of the curvature perturbation at the end of the non-attractor phase is given by

$$\mathcal{R}_\star = -\left(\frac{\delta\phi}{\Pi}\right)_\star, \quad \delta\phi(k) = \frac{H}{\sqrt{2k^3}}. \tag{2.3}$$

The corresponding power spectrum is flat. This might come as a surprise as slow-roll is badly violated, but in fact its a direct consequence of the dual symmetry described in ref. [55] (see also refs. [56–58]). We elaborate extensively on this point in appendix A. In a nutshell and alternatively, one can show it in the following way. Using the conformal time τ and setting $\mathcal{R} = u/z$, $z = (a\,\mathrm{d}\phi/\mathrm{d}\tau)/\mathcal{H}$, where $\mathcal{H}$ is the Hubble rate in conformal time, one can write the equation for the function u as (cf. eq. (A.2))

$$\frac{1}{u}\frac{\mathrm{d}^2 u}{\mathrm{d}\tau^2} = 2a^2H^2\left(1 + \frac{5}{2}\epsilon + \epsilon^2 - 2\epsilon\eta - \frac{1}{2}\frac{V_{,\phi\phi}}{H^2}\right) - k^2, \tag{2.4}$$

where ϵ and η are the slow-roll parameters defined in eq. (A.3) and a is the scale factor. Since during the non-attractor phase $\epsilon \ll 1$, $\eta \simeq 3$ and the potential is very flat, the right-hand side of the previous equation is approximated on super-Hubble scales to $2/\tau^2 \simeq (\mathrm{d}^2a/\mathrm{d}\tau^2)/a$

JCAP07(2018)032

and therefore $u \propto a$. It provides the standard solution for the mode function of the curvature perturbation

$$\mathcal{R}_k = \frac{\mathcal{H}}{(\mathrm{d}\phi/\mathrm{d}\tau)\sqrt{2k^3}}(1+ik\tau)e^{-ik\tau}. \tag{2.5}$$

This is the standard slow-roll solution with the crucial exception that the inflaton velocity changes rapidly with time. Notice also that the expression (2.3) can be extended at the end of inflation. This is possible if the transition from the non-attractor phase to the subsequent slow-roll phase (if any) is sudden, i.e. the velocity during the subsequent slow-roll phase is much bigger than $\Pi_\star$. Under these circumstances, the power spectrum does not have time to change and remains indeed (2.3) till the end of inflation [39]. We give more details in appendix B.

So far, we have discussed the perturbation associated to the modes which leave the Hubble radius deep in the non-attractor phase. However, the peak of the curvature perturbation is in fact reached for those modes which leave the Hubble radius during the sudden transition from the slow-roll phase into the non-attractor phase. During this transition the (would-be) slow-roll parameter $\eta = -\Pi'/\Pi$ jumps from a tiny value to 3.

To see what happens, we model the parameter η as $\eta \simeq 3\theta(\tau - \tau_0)$, where we have now turned again to conformal time τ. If so, and if we indicate by ϵ_+ the slow-roll parameter during the slow-roll phase preceding the non-attractor phase and assume it to be constant in time, one has

$$\mathcal{R}_k = \frac{H}{\sqrt{2\epsilon_+ k^3}}(1+ik\tau)e^{-ik\tau} \quad \text{for} \quad \tau < \tau_0, \tag{2.6}$$

and [39]

$$\left(\frac{\tau}{\tau_0}\right)^3 \mathcal{R}_k = \alpha_k \frac{H}{\sqrt{2k^3}}(1+ik\tau)e^{-ik\tau} + \beta_k \frac{H}{\sqrt{2k^3}}(1-ik\tau)e^{ik\tau} \quad \text{for} \quad \tau > \tau_0, \tag{2.7}$$

where we have taken into account that immediately after the beginning of the non-attractor phase the curvature perturbation increases as the inverse cubic power of the conformal time (cf. eq. (2.2)). Imposing continuity of the two functions together of their derivatives, one obtains a power spectrum at the end of inflation

$$\begin{aligned} \mathcal{P}_\mathcal{R} &= g(-k\tau_0)\,\mathcal{P}_{\mathcal{R}_\star}, \\ g(x) &= \frac{1}{2x^6}\left(9 + 18x^2 + 9x^4 + 2x^6 + 3(-3+7x^4)\cos 2x - 6x(3+4x^2-x^4)\sin 2x\right). \end{aligned} \tag{2.8}$$

The function $g(x)$ is $\mathcal{O}(x^4)$ for $x \simeq 0$, has a maximum of about 2.5 around $x \simeq 3$ and oscillates rapidly around 1 for $x \gg 1$. We can conclude that the power spectrum has the following shape: it increases, reaches a peak, and then decreases a bit till a plateau is encountered. This is in good agreement with what obtained, for instance, in refs. [57, 58]. The amplitude of the peak is about 2.5 times larger than the plateau in correspondence of the modes which leave the Hubble radius during the non-attractor phase

$$\mathcal{P}_{\mathcal{R}_{\mathrm{pk}}} \simeq 2.5\,\mathcal{P}_{\mathcal{R}_\star} = 2.5\left(\frac{H}{2\pi\Pi}\right)_\star. \tag{2.9}$$

Of course, given the assumption of sudden transition of η from tiny values to 3 around τ_0 and having assumed ϵ_+ constant, we expect this number to change by a factor $\mathcal{O}(1)$ depending

JCAP07(2018)032

upon the exact details. The linearisation of the potential is an approximation, but it captures the main features of the final result. For more complicated situations, for instance if during the non-attractor phase the inflation crosses an inflection point, one expects again a peak in the curvature perturbation for that mode leaving the Hubble radius at the sudden transition between the slow-roll and the non-attractor phase. However, one does not expect a significant plateau following the maximum as the non-attractor phase is typically very short. This also implies that the exact amplitude of the peak depends on the fine details of the transition.

An example: Starobinsky's model. In order to assess the quality of our findings we can consider Starobinsky's model [59] which is characterised by a potential with two linear regions

$$V(\phi) \simeq V_0 \left(1 + \sqrt{2\epsilon_+}(\phi - \phi_0)\right) + \cdots \quad \text{for} \quad \phi > \phi_0, \tag{2.10}$$

$$V(\phi) \simeq V_0 \left(1 + \sqrt{2\epsilon_-}(\phi - \phi_0)\right) + \cdots \quad \text{for} \quad \phi < \phi_0, \tag{2.11}$$

where $\epsilon_\pm$ are the slow-roll parameter during the slow-roll phase and the non-attractor phase, respectively. In fact, to deal with the problem numerically we have parametrised the discontinuity in the potential as

$$V(\phi) = V_0 \left(1 + \frac{1}{2}\left(\sqrt{2\epsilon_+} - \sqrt{2\epsilon_-}\right)(\phi - \phi_0)\tanh\left(\frac{\phi - \phi_0}{\delta}\right) + \frac{1}{2}\left(\sqrt{2\epsilon_+} + \sqrt{2\epsilon_-}\right)(\phi - \phi_0)\right), \tag{2.12}$$

where δ determines the size of the region in which the potential smoothly changes slope. If $\delta \ll 1$ the potential during the non-attractor phase becomes exactly linear. We will comment on the effect of varying δ on the quantum diffusion in section 4.

If $\epsilon_+ \gg \epsilon_-$, a prolonged non-attractor phase is obtained during which

$$\frac{\phi'}{\mathcal{H}} = -\sqrt{2\epsilon_-} - (\sqrt{2\epsilon_+} - \sqrt{2\epsilon_-})(\tau/\tau_0)^3. \tag{2.13}$$

The inflaton velocity at the beginning of the non-attractor phase is $-\sqrt{2\epsilon_+}$, then it quickly decays reaching a maximum (recall velocities are negative) at $(\tau_{\rm max}/\tau_0)^3 \simeq 2\sqrt{\epsilon_+/\epsilon_-}$ and then it reaches the value $-\sqrt{2\epsilon_+}$. The corresponding power spectrum in figure 2 illustrates three relevant points: the fact that the power spectrum reaches a plateau and becomes scale-independent, the amplitude of the plateau is reproduced by the standard slow-roll formula (see appendix A) and finally that the formula (2.8) provides a good fit to the numerical result.

Non-attractor: more physical cases. We turn now the discussion to more physical cases discussed recently in the literature. First, we consider the model in ref. [18]. Leaving aside the details of the particular string model giving rise to it, the inflaton potential reads

$$V(\phi) = \frac{{W_0}^2}{\mathcal{V}^3}\left[\frac{c_{\rm up}}{\sqrt[3]{\mathcal{V}}} + \frac{a_{\rm w}}{e^{\frac{\phi}{\sqrt{3}}} - b_{\rm w}} - \frac{c_{\rm w}}{e^{\frac{\phi}{\sqrt{3}}}} + \frac{e^{\frac{2\phi}{\sqrt{3}}}}{\mathcal{V}}\left(d_{\rm w} - \frac{g_{\rm w}}{r_{\rm w}e^{\sqrt{3}\phi}/\mathcal{V} + 1}\right)\right], \tag{2.14}$$

where the parameters used in our analysis can be found in table 1.

We have checked that they provide the correct CMB normalisation at large scales, as well as the correct spectral index and PBH abundance to match the dark matter abundance. The inflaton potential has an inflection point violating the slow-roll conditions, see figure 3, where the field is forced to enter a non-attractor phase which lasts a few e-folds and a boost

JCAP07(2018)032

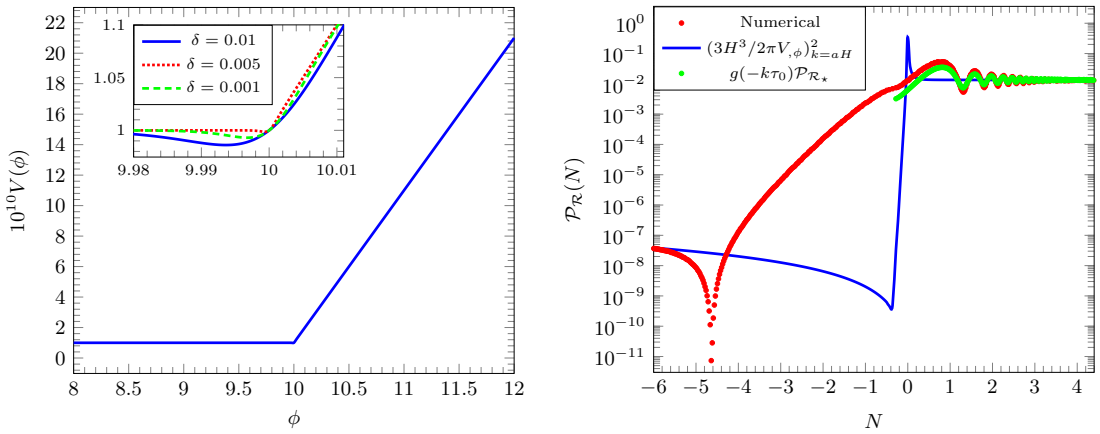

Figure 2. On the left, the Starobinsky's potential. On the right, the power spectrum in Starobinsky's model (not normalised at the CMB on large scales) obtained for $\epsilon_+/\epsilon_- = 10^8$ and as a function of N corresponding to $k = aH$. We have arbitrarily set $N = 0$ at the time at which η reaches 3.

$a_{\rm w}$	$b_{\rm w}$	$c_{\rm w}$	$d_{\rm w}$	$g_{\rm w}$	$r_{\rm w}$	$\mathcal{V}$	W_0	$c_{\rm up}$
0.02	1	0.04	0	$3.076278 \cdot 10^{-2}$	$7.071067 \cdot 10^{-1}$	1000	12.35	0.0382

Table 1. Parameter set for the string model in ref. [18].

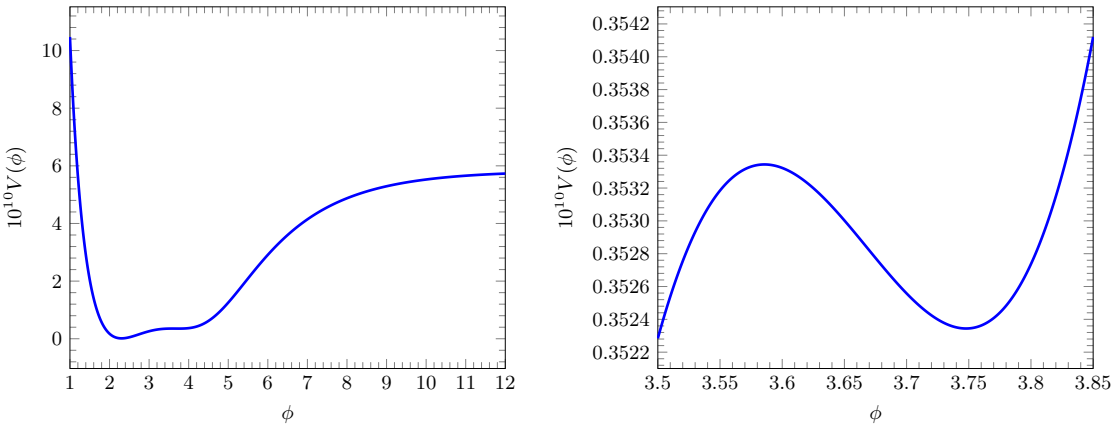

Figure 3. Inflaton potential from ref. [18] with parameter set defined in Tab 1. On the right hand side, the detail of the local minimum and maximum around the inflection point.

in the curvature power spectrum is generated. The solution to the Friedmann equations shows that the background evolution can be divided as follows. In a first stage the field experiences a slow-roll evolution compatible with the constraints on CMB scales. When the field approaches the local minimum, the fields enters a non-attractor phase where $\eta = 3$. After the following local maximum, the field exits the non-attractor phase leading to the end of the inflationary era.

We numerically solve the equation for the comoving curvature perturbation $\mathcal{R}$ (cf. eq. (A.1)) starting from the usual Bunch-Davies vacuum in the asymptotic region $(-k\tau) \gg 1$.

JCAP07(2018)032

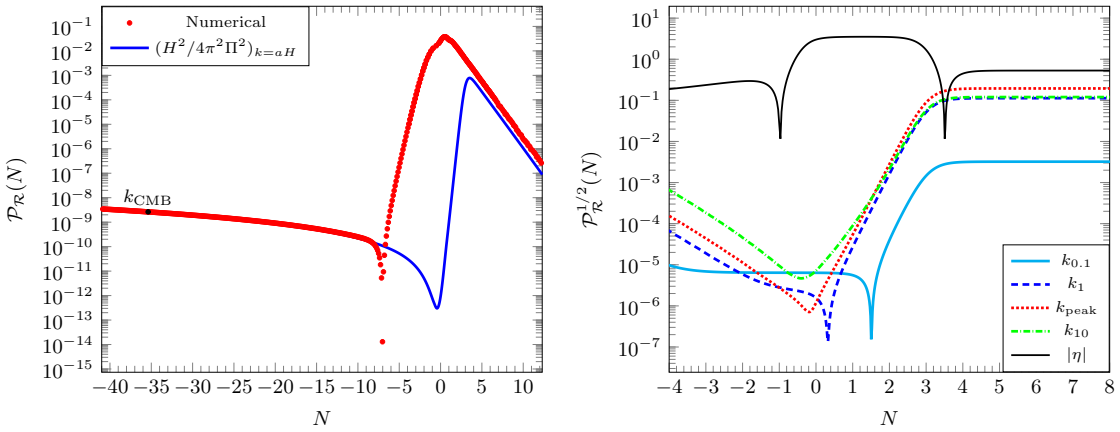

Figure 4. The left figure shows the power spectrum for the model in ref. [18] as a function of N corresponding to $k = aH$ and where we have arbitrarily set $N = 0$ at the time at which η reaches 3. Together with the numerical solution of the power spectrum in the region of interest, the slow-roll formula is plotted with the power spectrum computed at Hubble crossing. In the right figure the behaviour of η and of the different modes are shown. One can also observe that the transition of the parameter η from its slow-roll value to 3 lasts ~ 1 e-fold. Notice that the modes stop growing when the non-attractor phase ends, that is when the $z^{-1}\mathrm{d}z/\mathrm{d}\tau$ becomes positive again.

Figure 4 shows the power spectrum and the behaviour of the different modes. We have indicated by $k_{\rm pk}$ the mode leading to the largest amplitude and by k_1 the mode that leaves the Hubble radius at the transition point (approximately at $N \simeq -1$ in figure 4). We have called $k_{0.1}$ and k_{10} the wavenumbers respectively 0.1 and 10 times larger than k_1. We have also plotted the power spectrum computed at Hubble crossing to show its inadequacy in reproducing the exact result which must be calculated at the end of the non-attractor phase. Notice also that the curvature perturbation $\mathcal{R}_{\rm pk}$ grows until the end of the non-attractor phase, meaning that it takes advantage of the exponential decrease of the inflaton velocity until the end of the non-attractor phase, then it remains constant until the end of inflation. As we mentioned, this is because the transition back to the slow-roll phase is sudden and despite the fact that the parameter η does not go back immediately to very small values [39]. As for the absolute amplitude of the perturbation at the peak, we cannot really make use of the formula (2.3) since when the mode leaves the Hubble radius both ϵ and η change considerably. Numerically, we have estimated $\mathcal{P}^{1/2}_{\mathcal{R}_{\rm pk}} \simeq 7(H/2\pi\Pi_\star)$.

In the following we will also perform our analysis of the model in ref. [19]. The inflaton potential

$$V(\phi) = V_0 + \frac{1}{2}m^2\phi^2 + \Lambda_1^4\frac{\phi}{f}\cos\left(\frac{\phi}{f}\right) + \Lambda_2^4\sin\left(\frac{\phi}{f}\right) \tag{2.15}$$

is characterised by a series of oscillations around the quadratic potential, the last of which is capable of generating an inflection point, tuned such that the power-spectrum is enhanced as previously described for model [18], see figure 5. We have chosen to use the parameter set 1 in ref. [19] for our analysis for sake of comparison. Also for this case we have numerically estimated $\mathcal{P}^{1/2}_{\mathcal{R}_{\rm pk}} \simeq 7(H/2\pi\Pi_\star)$. The models in refs. [18, 19] are similar to those of other recent literature [15–17, 40] and we expect our analysis for the quantum diffusion to apply to those cases too.

JCAP07(2018)032

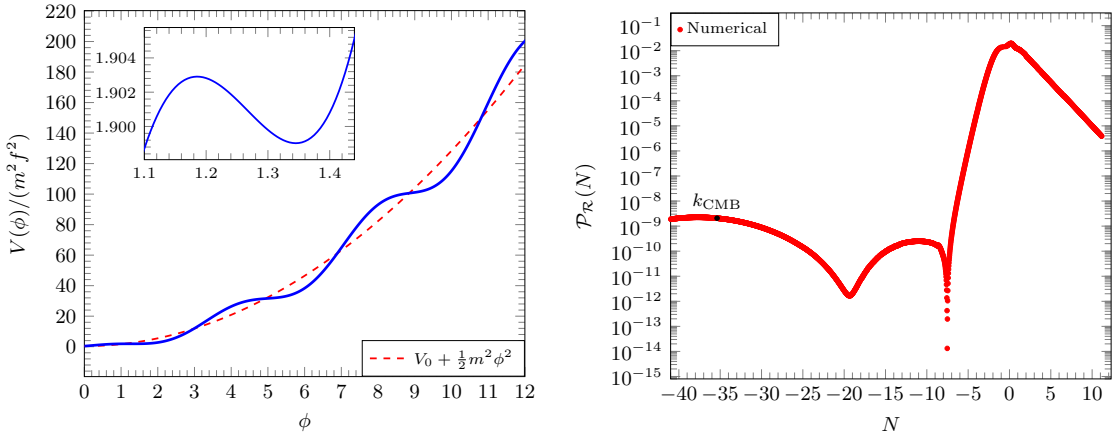

Figure 5. On the left, the potential (2.15) of ref. [19] compared to the quadratic potential. In the box, the detail of the potential near the inflection point. On the right, the corresponding power spectrum as a function of N corresponding to $k = aH$ and where we have arbitrarily set $N = 0$ at the time at which η reaches 3.

3 The non-attractor phase and quantum diffusion

Let us now come back to the role of quantum diffusion. If too large, quantum diffusion causes a loss of information as the curvature perturbation may not be reconstructed any longer at late times in terms of classical trajectories [17]. Different scales mix and the corresponding amplitude will be left undetermined for an observer at late times. Since quantum diffusion becomes more and more relevant as the field slows down and consequently the power spectrum grows, this clearly creates an issue and one expects a upper bound on the curvature perturbation in order for the quantum diffusion to be irrelevant.

Since the power spectrum is fixed by the inverse of the velocity of the inflaton field at the end of the non-attractor phase, we expect that, if the spread of the distribution of velocities caused by the stochastic motion is too large, then along most of the trajectories the perturbation will be either too large or to too small to generate PBHs in the allowed range of masses. One has therefore to find the amount of dispersion undergone by the velocity of the inflaton field.

Let us also notice that the power spectrum is growing during the non-attractor phase after the corresponding wavelength leaves the Hubble radius and therefore the issue of the quantum diffusion becomes more relevant at the end of the non-attractor phase. We will therefore discuss the criterion at the end of such a phase, where one expects the strongest constraints.

The stochastic equation (1.8) can be written as an Ornstein-Uhlenbeck process

$$\begin{aligned} \frac{\mathrm{d}\phi}{\mathrm{d}N} &= \Pi, \\ \frac{\mathrm{d}\Pi}{\mathrm{d}N} + 3\Pi + \frac{V_{,\phi}}{H^2} &= \xi, \\ \langle \xi(N)\xi(N')\rangle &= D\delta(N-N'), \\ D &= \frac{9H^2}{4\pi^2}, \end{aligned} \tag{3.1}$$

JCAP07(2018)032

where D is the diffusion coefficient. We may write the Kramers-Moyal (KM) equation for the corresponding probability $P(\phi, \Pi, N)$ as [53]

$$\frac{\partial P}{\partial N} = -\frac{\partial}{\partial \phi}(\Pi P) + \frac{\partial}{\partial \Pi}\left[\mathcal{V}_{,\Pi} P + \frac{V_{,\phi}}{H^2} P\right] + \frac{D}{2}\frac{\partial^2}{\partial \Pi^2} P, \tag{3.2}$$

where

$$\mathcal{V}(\Pi) = \frac{3}{2}\Pi^2. \tag{3.3}$$

The initial condition for the probability can be taken to be

$$P(\phi, \Pi, 0) = \delta_D(\phi - \phi_0)\delta_D(\Pi - \Pi_0), \tag{3.4}$$

as we assume that during the preceding slow-roll phase the motion is purely along classical trajectories.

Generic potential. We re-write the KM equation as

$$\begin{aligned} \frac{\partial P}{\partial N} &= L_{\rm KM}\, P = (L_{\rm rev} + L_{\rm ir})\; P, \\ L_{\rm rev} &= -\Pi\frac{\partial}{\partial \phi} + \frac{V_{,\phi}}{H^2}\frac{\partial}{\partial \Pi}, \\ L_{\rm ir} &= \frac{\partial}{\partial \Pi}\left(3\Pi + \frac{D}{2}\frac{\partial}{\partial \Pi}\right). \end{aligned} \tag{3.5}$$

The stationary solution for the operator $L_{\rm ir}$ is proportional to $\exp(-3\Pi^2/D)$ and we can generate a Hermitian operator

$$\overline{L}_{\rm ir} = \exp\left(\frac{3\Pi^2}{2D}\right) L_{\rm ir} \exp\left(-\frac{3\Pi^2}{2D}\right) = \overline{L}_{\rm ir}^{\dagger} = -3a^{\dagger}a, \tag{3.6}$$

where

$$a = \sqrt{\frac{D}{6}}\frac{\partial}{\partial \Pi} + \frac{\Pi}{2}\sqrt{\frac{6}{D}}, \quad a^{\dagger} = -\sqrt{\frac{D}{6}}\frac{\partial}{\partial \Pi} + \frac{\Pi}{2}\sqrt{\frac{6}{D}} \tag{3.7}$$

are the annihilation and creator operators with $[a, a\dagger] = 1$. To take advantage of this procedure, we also redefine the operator

$$\overline{L}_{\rm rev} = \exp\left(\frac{3\Pi^2}{2D} + \rho\frac{V}{H^2}\frac{6}{D}\right) L_{\rm rev} \exp\left(-\frac{3\Pi^2}{2D} - \rho\frac{V}{H^2}\frac{6}{D}\right) = -aA - a^{\dagger}\hat{A}, \tag{3.8}$$

where ρ is an arbitrary constant

$$A = \sqrt{\frac{D}{6}}\frac{\partial}{\partial \phi} - \rho\frac{V}{H^2}\sqrt{\frac{6}{D}}, \qquad \hat{A} = \sqrt{\frac{D}{6}}\frac{\partial}{\partial \phi} + (1-\rho)\frac{V}{H^2}\sqrt{\frac{6}{D}}, \tag{3.9}$$

with $[A, \hat{A}] = V_{\phi\phi}/H^2$. Now, the orthonormalised eigenfunctions of the operator $\overline{L}_{\rm ir}$, that is

$$\overline{L}_{\rm ir}\phi_n(\Pi) = -3n\phi_n(\Pi), \quad a^{\dagger}a\phi_n(\Pi) = n\phi_n(\Pi), \tag{3.10}$$

JCAP07(2018)032

are

$$\phi_n(\Pi) = (a^\dagger)^n \phi_0(\Pi)/\sqrt{n!}, \quad \phi_0(\Pi) = \frac{\exp\left(-3\Pi^2/2D\right)}{\sqrt{D/6\sqrt{2\pi}}}. \tag{3.11}$$

Since the operator $L_{\rm KM}$ is of the form

$$L_{\rm KM} = \exp\left(-\frac{3\Pi^2}{2D} - \rho\frac{V}{H^2}\frac{6}{D}\right)\left(\overline{L}_{\rm ir} + \overline{L}_{\rm rev}\right)\exp\left(\frac{3\Pi^2}{2D} + \rho\frac{V}{H^2}\frac{6}{D}\right)\phi_0^{-1}(\Pi), \tag{3.12}$$

or

$$L_{\rm KM} = -\phi_0(\Pi)\exp\left(-\rho\frac{V}{H^2}\frac{6}{D}\right)\left(3a^\dagger a + aA + a^\dagger\hat{A}\right)\exp\left(\rho\frac{V}{H^2}\frac{6}{D}\right)\phi_0^{-1}(\Pi), \tag{3.13}$$

we can expand the probability as [53]

$$P = \phi_0(\Pi)\exp\left(-\rho\frac{V}{H^2}\frac{6}{D}\right)\sum_{n\geq 0} c_n(\phi, N)\phi_n(\Pi), \tag{3.14}$$

so that the distribution in the inflaton field is only given by the first term of the expansion

$$\int \mathrm{d}\Pi\, P = \exp\left(-\rho\frac{V}{H^2}\frac{6}{D}\right)c_0(\phi, t), \tag{3.15}$$

where nevertheless the coefficients c_n satisfy the so-called Brinkman's hierarchy

$$\frac{\partial c_n}{\partial N} = -\sqrt{n}\hat{A}c_{n-1} - 3nc_n - \sqrt{n+1}Ac_{n+1} \tag{3.16}$$

and it is equivalent to the KM equation. This equation contains an infinite number of terms. For pedagogical purposes, let us truncate though the system by setting $c_n = 0$ for $n \geq 3$, so that the Brinkman's hierarchy reduces to

$$\begin{aligned} \frac{\partial c_0}{\partial N} + Ac_1 &= 0, \\ \frac{\partial c_1}{\partial N} + \hat{A}c_0 + 3c_1 &= 0. \end{aligned} \tag{3.17}$$

For a large friction term one can neglect the term $\partial c_1/\partial N$, and we could eliminate c_1 in favour of c_0. Setting $\rho = 0$, we find

$$\frac{\partial c_0}{\partial N} = -Ac_1 = \frac{1}{3}A\hat{A}c_0 = \frac{1}{3H^2}\frac{\partial}{\partial\phi}\left(V_{,\phi}c_0\right) + \frac{1}{2}\frac{D}{9}\frac{\partial^2 c_0}{\partial\phi^2}, \tag{3.18}$$

which is the standard Fokker-Planck equation. Had not we dropped the term $\partial c_1/\partial N$, we could have eliminated c_1 and get the equation for c_0

$$\frac{\partial^2 c_0}{\partial N^2} + 3\frac{\partial c_0}{\partial N} = \frac{1}{H^2}\frac{\partial}{\partial\phi}\left(V_{,\phi}c_0\right) + \frac{D}{6}\frac{\partial^2 c_0}{\partial\phi^2}, \tag{3.19}$$

which is Brinkman's equation. Retaining the coefficients c_n with $n \geq 3$ will introduce spatial derivatives higher than two. We find here what we mentioned in the introduction, that the KM contains an infinite tower of spatial derivatives of the effective probability of the inflaton field and, due to Pawula's theorem, it is not consistent to drop derivatives higher than two. In this sense, the Fokker-Planck equation is not the correct starting point.

In the case of a linear potential the operators A and $\hat{A}$ commute, while for a quadratic potential their commutator is a constant and the analysis is made it easier. We will consider these cases next.

JCAP07(2018)032

Linear potential. We consider first the linear potential (2.1) as a prototype. In such a case, the KM equation has an exact solution [53]

$$P(\phi,\Pi,N) = \frac{1}{2\pi\left(\mathrm{Det}\mathbf{M}\right)^{1/2}}\exp\left\{-1/2[\mathbf{M}^{-1}]_{\phi\phi}(\Delta\phi)^2 - [\mathbf{M}^{-1}]_{\phi\Pi}\Delta\phi\Delta\Pi - 1/2[\mathbf{M}^{-1}]_{\Pi\Pi}(\Delta\Pi)^2\right\}, \tag{3.20}$$

where

$$\begin{aligned}
\Delta\phi &= \phi - \phi(N),\\
\Delta\Pi &= \Pi - \Pi(N),\\
\langle\phi(N)\rangle &= \phi(N) = \phi_0 + \frac{1}{3}(\Pi_0 - \Pi) - \sqrt{2\epsilon_V}N,\\
\langle\Pi(N)\rangle &= \Pi(N) = \sqrt{2\epsilon_V}\left(e^{-3N} - 1\right) + \Pi_0 e^{-3N},
\end{aligned} \tag{3.21}$$

and

$$\begin{aligned}
\mathbf{M}_{\phi\phi} &= \frac{D}{54}\left(6N - 3 + 4e^{-3N} - e^{-6N}\right),\\
\mathbf{M}_{\phi\Pi} &= \frac{D}{18}\left(1 - e^{-3N}\right)^2,\\
\mathbf{M}_{\Pi\Pi} &= \frac{D}{6}\left(1 - e^{-6N}\right).
\end{aligned} \tag{3.22}$$

At times $N \gtrsim 1$, the probability becomes

$$P(\phi,\Pi,N) = \frac{1}{\Pi}\left(\frac{27}{2D^2N}\right)^{1/2}\exp\left[-\frac{9}{2DN}(\Delta\phi)^2\right]\exp\left[\frac{3}{DN}\Delta\phi\Delta\Pi\right]\exp\left[-\frac{3}{D}(\Delta\Pi)^2\right]. \tag{3.23}$$

Integrating over Π we obtain

$$P_\phi(\phi,N) = \frac{3}{\sqrt{2\pi DN}}\exp\left[-\frac{9}{2DN}(\phi - \phi(N))^2\right] \tag{3.24}$$

and

$$\langle(\Delta\phi)^2\rangle = \int \mathrm{d}\phi\,(\phi - \phi(N))^2\,P_\phi(\phi,N) = \frac{D}{9}N. \tag{3.25}$$

Conversely, integrating over the scalar field ϕ, one obtains

$$P_\Pi(\Pi,N) = \sqrt{\frac{3}{\pi D}}\exp\left[-\frac{3}{D}(\Pi - \Pi(N))^2\right] \tag{3.26}$$

and

$$\langle(\Delta\Pi)^2\rangle = \int \mathrm{d}\Pi\,(\Pi - \Pi(N))^2\,P_\Pi(\Pi,N) = \frac{D}{6}. \tag{3.27}$$

We conclude that when the average velocity of the inflaton field decays exponentially, its variance reaches quickly an asymptotic and stationary value given by eq. (3.27). There is an alternative way to obtain the same result. From the KM equation, we may derive the following set of equations

$$\begin{aligned}
\frac{\partial}{\partial N}\langle(\Delta\phi)^2\rangle &= 2\langle\Delta\phi\Delta\Pi\rangle,\\
\frac{\partial}{\partial N}\langle\Delta\phi\Delta\Pi\rangle &= \langle(\Delta\Pi)^2\rangle - 3\langle\Delta\phi\Delta\Pi\rangle,\\
\frac{\partial}{\partial N}\langle(\Delta\Pi)^2\rangle &= -6\langle(\Delta\Pi)^2\rangle + D.
\end{aligned} \tag{3.28}$$

JCAP07(2018)032

At times larger than a few Hubble times, the correlators involving $\Delta\Pi$ decay promptly to their equilibrium values $\langle\Delta\phi\Delta\Pi\rangle = 1/3\langle(\Delta\Pi)^2\rangle = D/18$ resulting in

$$\frac{\partial}{\partial N}\langle(\Delta\phi)^2\rangle = \frac{D}{9}, \tag{3.29}$$

reproducing (3.25) and (3.27).

Linear plus quadratic potential. Our considerations can be extended beyond the linear order in the potential. Let us expand the potential including the quadratic order

$$V(\phi) = V_0\left[1 + \sqrt{2\epsilon_V}(\phi-\phi_0) + \frac{1}{2}\eta_V(\phi-\phi_0)^2\right] + \cdots, \tag{3.30}$$

where $\eta_V = V_{,\phi\phi}/3H^2$ parametrises the second derivative of the potential. The equation of motion leads to a classical value

$$\langle\Pi(N)\rangle = \Pi(N) \simeq \Pi_0 e^{-3N}\left(1 + \frac{1}{3}\eta_V + \frac{\sqrt{2\epsilon_V}}{\Pi_0}\right) - \Pi_0 e^{-\eta_V N}\left(\frac{1}{3}\eta_V + \frac{\sqrt{2\epsilon_V}}{\Pi_0}\right). \tag{3.31}$$

In particular, if one has a potential where ϕ_0 corresponds to a minimum and only the quadratic piece is there in the Taylor expansion one finds

$$\langle\Pi(N)\rangle = \Pi(N) \simeq \Pi_0 e^{-3N}\left(1 + \frac{1}{3}\eta_V\right) - \frac{\Pi_0}{3}\eta_V e^{-\eta_V N}. \tag{3.32}$$

In order to simplify the problem, we notice that in the stochastic equation of motion of the inflaton field

$$\frac{\mathrm{d}^2\phi}{\mathrm{d}N^2} + 3\frac{\mathrm{d}\phi}{\mathrm{d}N} + 3\sqrt{2\epsilon_V} + 3\eta_V(\phi-\phi_0) = \xi, \tag{3.33}$$

one can shift the field Π by an amount $-3\sqrt{2\epsilon_V}$ and ϕ by an amount $-3\sqrt{2\epsilon_V}N$ in order to get rid of the constant force. The problem reduces for this shifted field to the following set of equations (we do not redefine the fields to avoid cluttering notation)

$$\begin{aligned}\frac{\mathrm{d}\phi}{\mathrm{d}N} &= \Pi,\\ \frac{\mathrm{d}\Pi}{\mathrm{d}N} + 3\Pi + 3\eta_V\phi &= \xi.\end{aligned} \tag{3.34}$$

The solution of these equations is again given in eq. (3.20). This time however

$$\begin{aligned}\phi(N) &= [\exp(-\mathbf{A}N)]_{\phi\phi}\phi_0 + [\exp(-\mathbf{A}N)]_{\phi\Pi}\Pi_0,\\ \Pi(N) &= [\exp(-\mathbf{A}N)]_{\Pi\phi}\phi_0 + [\exp(-\mathbf{A}N)]_{\Pi\Pi}\Pi_0,\\ \mathbf{A} &= \begin{pmatrix}0 & -1\\ 3\eta_V & 3\end{pmatrix}.\end{aligned} \tag{3.35}$$

Also, by defining

$$\lambda_{1,2} = \frac{1}{2}\left(3 \pm \sqrt{9-12\eta}\right), \quad \lambda_1 \simeq 3, \quad \lambda_2 \simeq \eta_V, \tag{3.36}$$

JCAP07(2018)032

one obtains [53]

$$\begin{aligned}
\mathbf{M}_{\phi\phi} &= \frac{D}{2(\lambda_1-\lambda_2)^2}\left[\frac{\lambda_1+\lambda_2}{\lambda_1\lambda_2}+\frac{4}{\lambda_1+\lambda_2}\left(e^{-(\lambda_1+\lambda_2)N}-1\right)-\frac{1}{\lambda_1}e^{-2\lambda_1 N}-\frac{1}{\lambda_2}e^{-2\lambda_2 N}\right],\\
\mathbf{M}_{\phi\Pi} &= \frac{D}{2(\lambda_1-\lambda_2)^2}\left(e^{-\lambda_1 N}-e^{-\lambda_2 N}\right)^2,\\
\mathbf{M}_{\Pi\Pi} &= \frac{D}{2(\lambda_1-\lambda_2)^2}\left[\lambda_1+\lambda_2+\frac{4\lambda_1\lambda_2}{\lambda_1+\lambda_2}\left(e^{-(\lambda_1+\lambda_2)N}-1\right)-\lambda_1 e^{-2\lambda_1 N}-\lambda_2 e^{-2\lambda_2 N}\right],
\end{aligned} \tag{3.37}$$

or

$$\begin{aligned}
\mathbf{M}_{\phi\phi} &= \frac{D}{18}\left[\frac{1}{3}+\frac{1}{\eta_V}+\frac{4}{3}\left(e^{-3N}-1\right)-\frac{1}{3}e^{-6N}-\frac{1}{\eta_V}e^{-2\eta_V N}\right],\\
\mathbf{M}_{\phi\Pi} &= \frac{D}{18}\left(e^{-3N}-e^{-\eta_V N}\right)^2,\\
\mathbf{M}_{\Pi\Pi} &= \frac{D}{18}\left[3+4\eta_V\left(e^{-3N}-1\right)-3e^{-6N}-\eta_V e^{-2\eta_V N}\right].
\end{aligned} \tag{3.38}$$

At large times and for small η_V they reduce to

$$\begin{aligned}
\mathbf{M}_{\phi\phi} &= \frac{D}{18}\left[\frac{1}{\eta_V}\left(1-e^{-2\eta_V N}\right)-1\right],\\
\mathbf{M}_{\phi\Pi} &= \frac{D}{18}e^{-2\eta_V N},\\
\mathbf{M}_{\Pi\Pi} &= \frac{D}{18}\left(3-\eta_V e^{-2\eta_V N}\right).
\end{aligned} \tag{3.39}$$

For $\eta_V > 0$, i.e. for a harmonically bound state, in the large time limit one obtains a stationary solution. However, for $\eta_V < 0$, i.e. for an inverted parabolic potential, the force felt by the inflaton is repulsive. In both cases, the width of the distribution of the inflaton velocities obtained integrating out over all possible values of the inflaton field reads

$$\langle(\Delta\Pi)^2\rangle \simeq \frac{D}{18}\left(3-\eta_V e^{-2\eta_V N}\right). \tag{3.40}$$

In the model of refs. [18, 19] the plateau is in fact a region around an inflection point between a minimum and a maximum so that η_V changes sign from positive to negative (if the minimum is encountered first). Being the dynamics more complex than what described above, we should expect deviations of order unity from our estimate.

4 Numerical analysis of quantum diffusion

In this section we present the numerical studies we performed in order to check the validity of our analytical findings. We have numerically solved the system (3.1) with the available Mathematica routines for the solution of stochastic differential equations. We focus only on the inflaton velocity since the perturbations are sensitive to it. The spread in the inflaton field, which acquires typically Planckian values (at least in the vast majority of the literature) is irrelevant. At any rate, we have numerically checked that our numerical results coincide with this statement. We were able to test the robustness of our numerical implementation for the case of the linear potential, for which we have the analytical solution, eq. (3.20).

JCAP07(2018)032

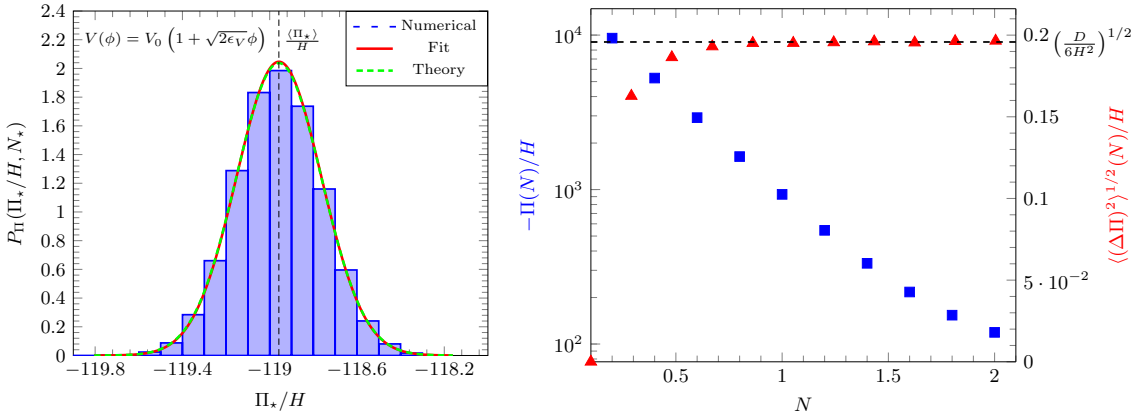

Figure 6. On the left, the numerical, the fit to numerical and the theoretical prediction for the probability $P_\Pi(\Pi_\star, N_\star)$ for the case of a linear potential with $\epsilon_V = 10^{-7}$. On the right, the classical evolution of $\Pi(N)$ together with the spread $\langle(\Delta\Pi)^2\rangle^{1/2}$ which stabilises at $(D/6)^{1/2}$ for $N \gtrsim 1$. It was checked numerically that changing the initial condition for $\Pi(0)$ by order of magnitudes does not give rise to significant modification of $\langle(\Delta\Pi)^2\rangle^{1/2}$ for $N < 1$. Furthermore, the plateau's value is not sensitive to the initial conditions, confirming the analytical result in eq. (3.27).

Linear potential and Starobinsky's model. We start by checking the solution of the KM equation in the case of a linear potential. Since we are interested in the dispersion of $\Pi_\star$ around its classical value, we recover numerically its variance among many realizations of the stochastic evolution.

In figure 6, one can see the comparison between the prediction (3.27) and the numerical results. The numerical results, obtained integrating over the inflaton field positions (whose spread is however tiny with respect to the average classical position), fully reproduce the analytical results (to the extent that the red line of the fit and the green one representing the theory overlap perfectly). We have also repeated our analysis for Starobinsky's model [59] we have introduced in section 2. The results are in figure 7 which show that the spread of the velocity approaches $(D/6)^{1/2}$. For smaller values of δ, the agreement with the linear potential result would be extended to the whole non-attractor phase, but the choice of δ is limited by numerical precision.

More physical cases. Having established that the numerical and analytical results agree for the simple case of the linear potential, we now turn our attention to more realistic cases discussed in the literature. As a representative example of the models in the literature, we consider the ones described in ref. [18] and [19] already introduced in section 2. We solve numerically the stochastic equations (3.1) setting up initial conditions deep enough in the slow-roll phase. It was checked that, as expected, the stochastic noise can be neglected throughout the entire slow-roll phase. We focus our attention on the dynamics during the non-attractor phase.

In figure 8 and figure 9 one can observe the evolution of $\Pi(N)$ and its dispersion around the mean value along the non-attractor phase, where the number of e-folds is set to zero at the transition. The procedure followed for the marginalisation over the $\phi(N)$ field is the same as the one previously presented for the case of a linear potential.

JCAP07(2018)032

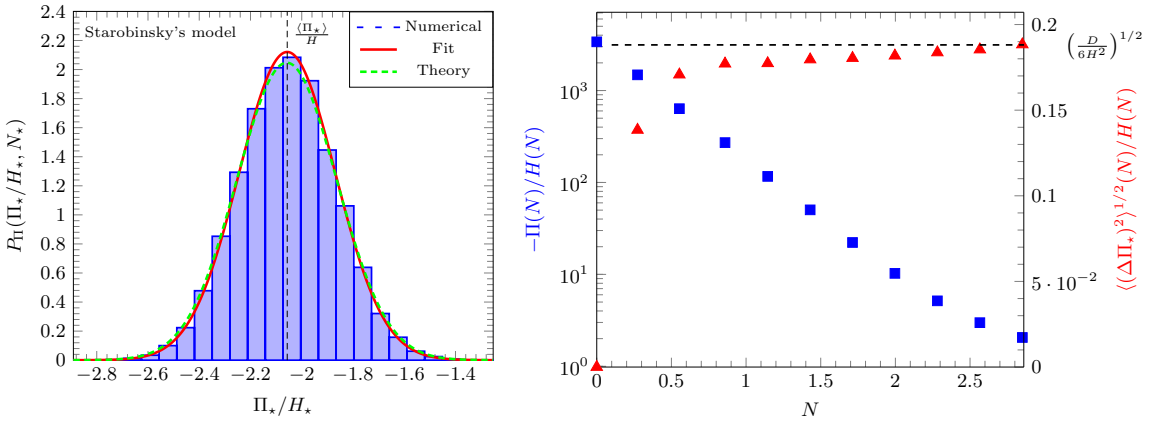

Figure 7. The numerical, the fit to numerical and the theoretical prediction for the probability $P_\Pi(\Pi_\star, N_\star)$ for the case of Starobinsky's model with $\delta = 0.01$ and $\epsilon_+/\epsilon_- = 10^8$. On the right, the classical evolution of $\Pi(N)$ together with the spread $\langle(\Delta\Pi)^2\rangle^{1/2}$ which tends towards $(D/6)^{1/2}$. We have used the same parameters as in section 2 and performed $5 \cdot 10^4$ realisations of the stochastic evolution.

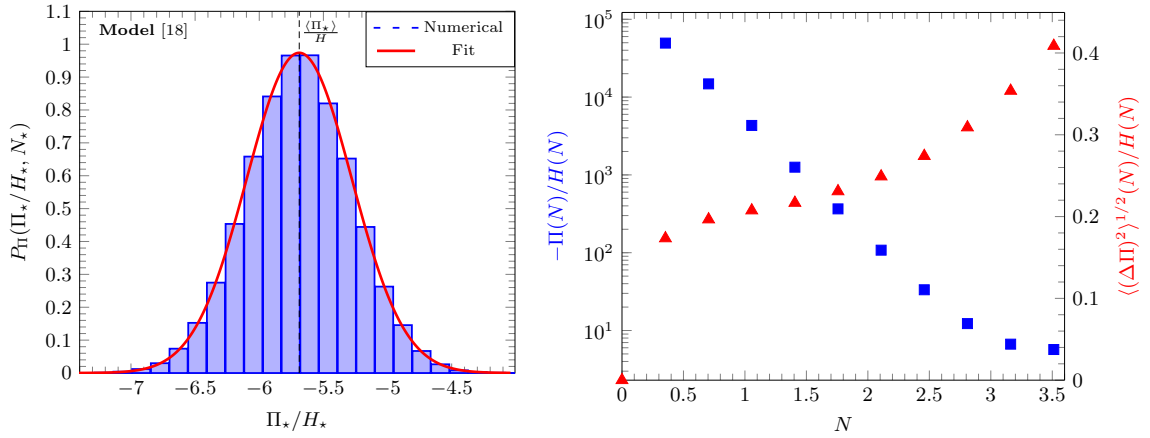

Figure 8. On the left the velocity probability obtained numerically together with its fit. On the right the evolution with time of the classical value of the velocity and its spread during the non-attractor phase. Calculations done for the model in ref. [18] with the parameter set in table 1. The results are based on $5 \cdot 10^4$ realisations of the stochastic evolution.

We see that the more the classical value of the inflaton velocity decreases, the more its spread grows with time. The distribution is well-fitted by a Gaussian with spread $\langle(\Delta\Pi)^2\rangle(N)$. In the former model, for example, at the end of the non-attractor phase, we have

$$\frac{\langle(\Delta\Pi)^2\rangle^{1/2}}{H} \simeq 0.4, \tag{4.1}$$

which is larger than about a factor of two than the variance for the linear potential $\sqrt{D/6}/H \simeq 0.2$. We notice instead that the behaviour of the spread is well reproduced by the expression (3.40) even though with deviations near the end of the non-attractor phase.

JCAP07(2018)032

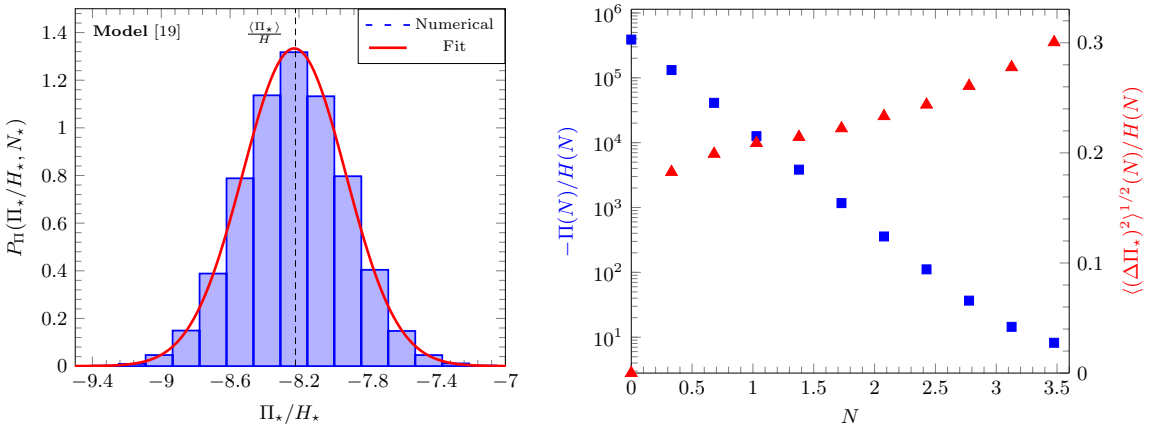

Figure 9. Same as figure 8, but for ref. [19], case 1.

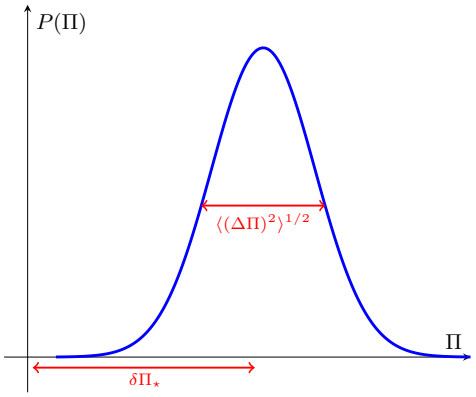

Figure 10. A representative behaviour of the quantum diffusion issue. The spread of the inflaton velocity probability $\langle(\Delta\Pi)^2\rangle^{1/2}$ has to be smaller than the distance between the origin and the average value of the velocity.

5 A criterion for the quantum diffusion

As previously discussed, the crucial quantity is the spread of the velocity $\Delta\Pi$ of the inflaton field for the various trajectories. If the spread of the probability distribution $\langle(\Delta\Pi)^2\rangle^{1/2}$ is smaller than the size $\delta\Pi_\star$ of the region over which the perturbation is of the order of $\mathcal{P}_{\mathcal{R}_{\rm pk}}^{1/2}$, then an insignificant part of the wave packet goes out the region where the curvature perturbation is $\mathcal{P}_{\mathcal{R}_{\rm pk}}^{1/2}$ and most of the trajectories will have the same curvature perturbation $\sim \mathcal{P}_{\mathcal{R}_{\rm pk}}^{1/2}$. We impose therefore the criterion that the spread of the probability distribution is still within the region where $\mathcal{P}_{\mathcal{R}}^{1/2} \sim \mathcal{P}_{\mathcal{R}_{\rm pk}}^{1/2}$, see figure 10,

$$\frac{\langle(\Delta\Pi)^2\rangle^{1/2}}{H} \ll \frac{\delta\Pi_\star}{H}, \tag{5.1}$$

JCAP07(2018)032

Linear potential. For the linear potential during the non-attractor phase, the region where the curvature perturbation has a given value $\mathcal{P}_{\mathcal{R}_{\rm pk}}^{1/2}$ has a width (recall that $\mathcal{P}_{\mathcal{R}_{\rm pk}} \sim 2.5\mathcal{P}_{\mathcal{R}_\star}$)

$$\delta\Pi_\star \simeq 1.6\frac{H}{2\pi\mathcal{P}_{\mathcal{R}_{\rm pk}}^{1/2}}. \tag{5.2}$$

and therefore one obtains the criterion

$$\mathcal{P}_{\mathcal{R}_{\rm pk}}^{1/2} \ll 1.6\frac{H}{2\pi\langle(\Delta\Pi)^2\rangle^{1/2}}. \tag{5.3}$$

If satisfied, we can conclude that along most of the classical trajectories PBH's can be generated. If not true, this is equivalent to say that the wave-function of the inflaton velocity penetrates into the regions where the velocities are much different from $\Pi_\star$, leading to non-perturbative values of $\mathcal{R}$ and to a totally random motion if $\Pi_\star \sim 0$. Of course, one can get a stronger constraint if one imposes that the penetration does not occur at p variances, or

$$\mathcal{P}_{\mathcal{R}_{\rm pk}}^{1/2} \ll 1.6\frac{H}{2p\pi\langle(\Delta\Pi)^2\rangle^{1/2}}. \tag{5.4}$$

Now, since

$$\sqrt{\frac{D}{6}} \ll \delta\Pi_\star, \tag{5.5}$$

we finally obtain

$$\mathcal{P}_{\mathcal{R}_{\rm pk}}^{1/2} \ll 1.6\sqrt{\frac{2}{3p^2}} \simeq \frac{1.3}{p}. \tag{5.6}$$

More physical cases. For the more realistic models discussed in refs. [18, 19] our results are provided in figures 8 and 9. As we have noticed, the distribution is well-fitted by a Gaussian with spread $\langle(\Delta\Pi)^2\rangle(N)$. As already mentioned, one needs to take the value of the curvature perturbation at the peak at the end of the non-attractor phase since the corresponding mode does not change in time afterwards. Therefore, taking into account that for both cases $\mathcal{P}_{\mathcal{R}_{\rm pk}}^{1/2} \simeq 7(H/2\pi\Pi_\star)$, we obtain

$$\frac{\delta\Pi_\star}{H} \simeq 1.4, \tag{5.7}$$

while

$$\frac{\langle(\Delta\Pi)^2\rangle^{1/2}}{H} \simeq 0.4, \tag{5.8}$$

which is comfortably smaller than (5.7). The criterion is well satisfied thanks to the boost the power spectrum gets at the peak with respect to the power spectrum calculated for the wavelength leaving the Hubble radius deep in the non-attractor phase. However, as we will see next, this does not seem enough for the quantum diffusion not to have an impact on the PBH abundance.

JCAP07(2018)032

6 A stronger criterion for the quantum diffusion

The presence of sizeable quantum diffusion enters in another relevant consideration and provides a stronger criterion. Assume a Gaussian form for the PBH mass function

$$\beta_{\rm prim}(M) \simeq \frac{\sigma_{\mathcal{R}}}{\sqrt{2\pi}\mathcal{R}_c} e^{-\mathcal{R}_c^2/2\sigma_{\mathcal{R}}^2}. \tag{6.1}$$

Suppose one fine-tunes the parameters of the inflaton potential to produce the right amount of PBH as dark matter, but without accounting for the quantum diffusion and therefore the spread of the inflaton velocities.

Practitioners of the production of PBHs as dark matter in single-field models of inflation know that a considerable fine-tuning is needed in any model to produce the right amount of dark matter in the form of PBHs. Any deviation from the fine-tuned set of parameters due to the uncertainty caused by the quantum diffusion will lead to huge variations of the PBH primordial mass fraction (as well as the ignorance on the non-Gaussian corrections do). Let us take therefore into account the spread now on the PBH mass fraction itself.

Linear potential. Assuming that $\sigma_{\mathcal{R}} \simeq \mathcal{P}_{\mathcal{R}_{\rm pk}}^{1/2} \sim (H/2\pi\Pi_\star)$, the PBH mass fraction has an average induced by quantum diffusion equal to

$$\langle \beta_{\rm prim}(M) \rangle = \int {\rm d}\Pi P_\Pi(\Pi)\, \beta_{\rm prim}(M)|_{\rm Gaussian}\,. \tag{6.2}$$

Using a Gaussian distribution for $\Pi_\star$ with spread $\langle(\Delta\Pi)^2\rangle^{1/2}$, we get

$$\langle \beta_{\rm prim}(M) \rangle = \frac{H^3\sigma_{\mathcal{R}}}{\sqrt{2\pi}\left(H^2 + 4\pi^2\mathcal{R}_c^2\langle(\Delta\Pi)^2\rangle\right)^{3/2}\mathcal{R}_c} e^{-\frac{H^2\mathcal{R}_c^2}{2\left(H^2+4\pi^2\mathcal{R}_c^2\langle(\Delta\Pi)^2\rangle\right)\sigma_{\mathcal{R}}^2}}. \tag{6.3}$$

Notice that the average value of the PBH primordial abundance gets shifted with respect to the expression (6.1) precisely because the distribution of the inflaton velocity has a nonvanishing width.

We may define a fine-tuning parameter $\Delta_{\rm qd}$ defined through the ratio of the averaged mass fraction in the presence of diffusion and the mass fraction in the absence of diffusion as

$$\frac{\langle \beta_{\rm prim}(M) \rangle}{\beta_{\rm prim}(M)} = e^{\Delta_{\rm qd}}. \tag{6.4}$$

Essentially, this fine-tuning parameter says how far is the average of the distribution of $\beta_{\rm prim}(M)$ from the classical value computed in the absence of quantum diffusion. We find that

$$\Delta_{\rm qd} \simeq -\frac{\mathcal{R}_c^2}{2\sigma_{\mathcal{R}}^2}\left(\frac{\varepsilon}{1+\varepsilon}\right), \quad \varepsilon = -\frac{4\pi^2\mathcal{R}_c^2\langle(\Delta\Pi)^2\rangle}{H^2}. \tag{6.5}$$

Imposing that the calculation is done in the absence of diffusion is trustable requires $|\Delta_{\rm qd}| \lesssim 1$, or

$$\frac{\langle(\Delta\Pi)^2\rangle^{1/2}}{H} \lesssim \frac{\sigma_{\mathcal{R}}}{\sqrt{2}\pi\mathcal{R}_c^2} \simeq 10^{-2}\left(\frac{\sigma_{\mathcal{R}}}{0.1}\right)\left(\frac{1.3}{\mathcal{R}_c}\right)^2. \tag{6.6}$$

For a linear potential this bound is violated by the fact that the spread in the velocity is $\sqrt{D/6}/H \simeq 0.2$. One might think to reduce the fine-tuning by, for instance, decrease the

JCAP07(2018)032

value of $\mathcal{R}_c$, however one should also recall that in order to get the right amount of dark matter in the form of PBH, $\beta_{\rm prim} \simeq 10^{-16}$, one needs $\sigma_{\mathcal{R}}/\mathcal{R}_c \sim 1/8$ and therefore decreasing $\mathcal{R}_c$ leads to a strong decrease in $\sigma_{\mathcal{R}}$. Alternatively, one can fix the spread in the velocity to be $\sqrt{D/6}/H \simeq 0.2$ and, imposing $|\Delta_{\rm qd}| \lesssim 1$, find a lower bound on the square root of the variance

$$\sigma_{\mathcal{R}} \gtrsim \frac{2}{\sqrt{3}}\mathcal{R}_c^2 \simeq 2\left(\frac{\mathcal{R}_c}{1.3}\right)^2, \tag{6.7}$$

which signals the difficulty of avoiding the impact of the quantum noise.

Non-attractor: more physical cases. For a more realistic potential, like the one in ref. [18], we have seen that the spread in the velocities at the end of the non-attractor phase is as large as $\langle(\Delta\Pi)^2\rangle^{1/2}/H \simeq 0.4$. To assess the impact of the quantum diffusion on the PBH abundance, we have proceeded as follows. We have set the parameters of the model as in section 2, see table 1, in such a way to reproduce the right abundance for the PBHs to be dark matter and for the potential to be consistent with the CMB constraints on the power spectrum at the reference scale of $k_{\rm CMB} = 0.05\,{\rm Mpc}^{-1}$ (the spectral index and the tensor to scalar ratio computed in the slow-roll region are as well in agreement with current data).

The PBH abundance has been calculated using the density contrast $\Delta(\vec{x}) = (4/9a^2H^2)\nabla^2\zeta(\vec{x})$ with threshold $\Delta_c \simeq 0.45$ [26] where the variance is defined as

$$\sigma_\Delta^2(R_H) = \frac{16}{81}\int_0^\infty {\rm d}\ln q (qR_H)^4 W^2(qR_H)\mathcal{P}_{\mathcal{R}}(q), \tag{6.8}$$

where $W(qR_H)$ is a Gaussian window function smoothing out the density contrast on the comoving horizon length $R_H = 1/aH$. The Gaussian approximation of the primordial mass fraction

$$\beta_{\rm prim}(M) \simeq \frac{\sigma_\Delta}{\sqrt{2\pi}\Delta_c} e^{-\Delta_c^2/2\sigma_\Delta^2}, \tag{6.9}$$

gives $\beta_{\rm prim}(10^{-15}M_\odot) \simeq 3\cdot 10^{-16}$ and therefore the right dark matter abundance. We have then included the quantum diffusion, run 10^4 realisations of the stochastic background evolution and for each of them we have calculated the primordial PBH abundance $\beta^{\rm qd}_{\rm prim}$.

Our results show that $\ln\beta^{\rm qd}_{\rm prim}$ is approximately Gaussian distributed around the value of $\beta^{\rm cl}_{\rm prim}$ computed using the classical inflaton evolution, and with a standard deviation $\sigma_{\beta^{\rm qd}_{\rm prim}}$, see figure 11. This is only an approximation because there is a small skewness shifting the average slightly away from its classical value. This means that $\beta^{\rm qd}_{\rm prim}$ is nearly distributed as a log-normal distribution. Extending what we have done previously, we can introduce a fine-tuning parameter defined to be

$$\Delta_{\rm qd} = \ln\frac{\beta^{\rm qd}_{\rm prim}}{\beta^{\rm cl}_{\rm prim}}. \tag{6.10}$$

This quantity is distributed like a Gaussian and is a measure of how close the distribution of the PBH mass fraction is peaked around the classical value. Therefore $\Delta_{\rm qd}$ is (nearly) centered around zero and within $p\sigma_{\beta^{\rm qd}_{\rm prim}}$ it acquires values

$$-p\sigma_{\beta^{\rm qd}_{\rm prim}} \lesssim \Delta_{\rm qd}(p) \lesssim p\sigma_{\beta^{\rm qd}_{\rm prim}}. \tag{6.11}$$

The values of $\Delta_{\rm qd}(p)$ are summarised in table 2. Notice that the range is not totally symmetric because of the small skewness. We observe that the criterion $|\Delta_{\rm qd}| \lesssim 1$ is grossly violated and

JCAP07(2018)032

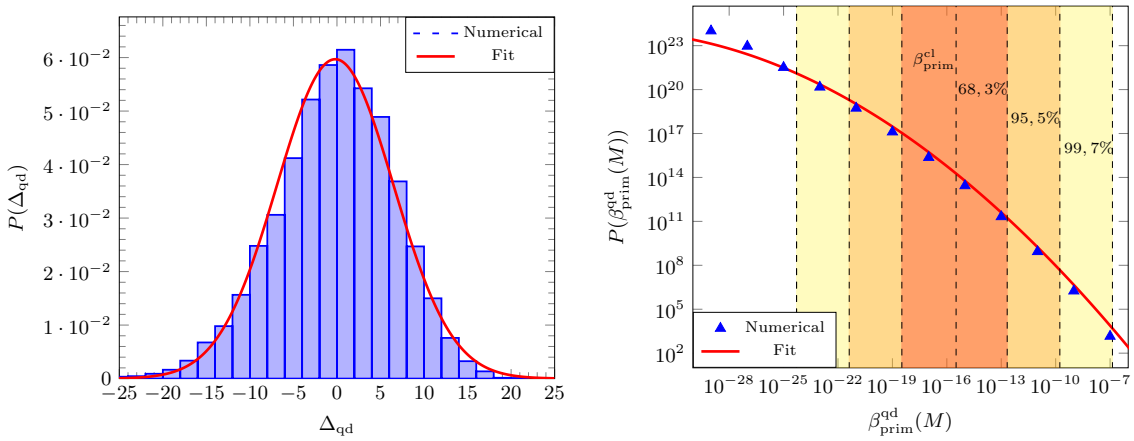

Figure 11. The probability density of $\Delta_{\rm qd}$, which is nearly Gaussian distributed around the classical value determined ignoring quantum diffusion, and of $\beta^{\rm qd}_{\rm prim}$ for model in ref. [18]. The results are derived from 10^4 realisations of the stochastic evolution.

Model [18]	$p=1$	$p=-1$	$p=2$	$p=-2$	$p=3$	$p=-3$
$\Delta_{\rm qd}(p)$	-6.49	6.88	-13.17	13.56	-19.85	20.25
$\beta^{\rm qd}_{\rm prim}(p)$	$2.13\cdot10^{-13}$	$3.33\cdot10^{-19}$	$1.70\cdot10^{-10}$	$4.16\cdot10^{-22}$	$1.36\cdot10^{-7}$	$5.20\cdot10^{-25}$
Model [19]	$p=1$	$p=-1$	$p=2$	$p=-2$	$p=3$	$p=-3$
$\Delta_{\rm qd}(p)$	-4.20	4.36	-8.48	8.64	-12.76	12.92
$\beta^{\rm qd}_{\rm prim}(p)$	$7.33\cdot10^{-15}$	$1.41\cdot10^{-18}$	$5.29\cdot10^{-13}$	$1.95\cdot10^{-20}$	$3.81\cdot10^{-11}$	$2.70\cdot10^{-22}$

Table 2. Detailed values of the $\Delta_{\rm qd}(p)$ as defined in eq. (6.11) and their corresponding values of $\beta_{\rm prim}$ for models [18, 19].

the value of $\beta^{\rm qd}_{\rm prim}(M)$ violently deviates from the classical value due to the effect of quantum diffusion on the evolution of the background. In other words the values of the PBH mass fraction violently fluctuate around an average which is very different from the classical value thought to be needed to get the right abundance of the dark matter in the form of PBH.

Similar results are obtained for the model in ref. [19], they are shown in figure 12. For the sake of comparison we have used the same reference values as in ref. [19]. We notice that the dispersion of $\beta_{\rm prim}(M)$ is less prominent. However, this is only due to the fact that in ref. [19] a smaller threshold, $\Delta_c \simeq 0.3$, has been adopted, leading to smaller values of the variances to reproduce the right amount of dark matter in the form of PBHs. As a consequence, the impact of quantum diffusion is relatively smaller. Still, the criterion is violated as we can see from table 2. We also remark that higher values of $\Delta_c = (0.4-0.7)$ [26] are used in the literature and therefore even larger values of $\Delta_{\rm qd}$ will be obtained.

Our results make us confident that, while in principle conclusions might depend on the exact values of the square root of the variance σ_Δ and threshold Δ_c, the corresponding $|\Delta_{\rm qd}|$ will in general be too large. This is because changing the parameters of the model to get new variances with some new thresholds does not reduce significantly the spread of $\ln\beta_{\rm prim}$. Therefore, while our results are specific of the models we have considered, we believe the

JCAP07(2018)032

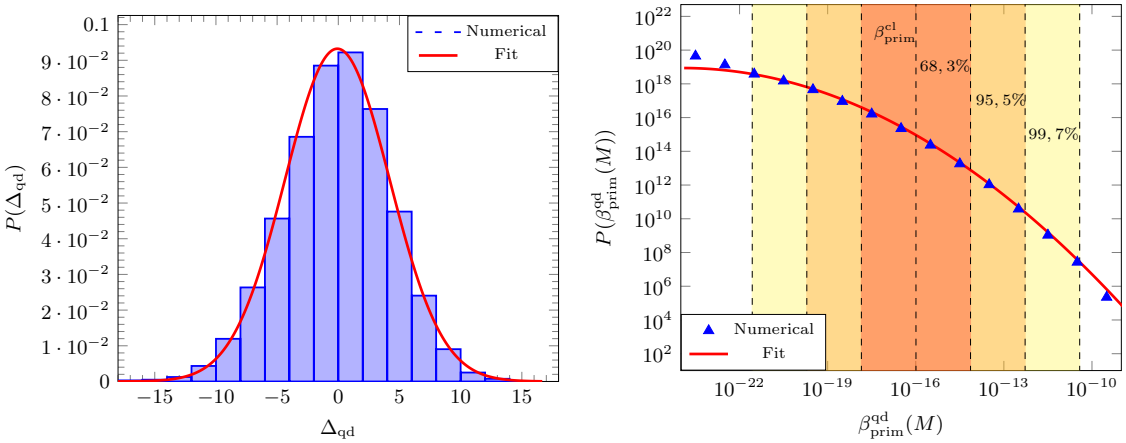

Figure 12. The probability density of $\Delta_{\rm qd}$, which is nearly Gaussian distributed around the classical value determined ignoring quantum diffusion, and of $\beta^{\rm qd}_{\rm prim}$ for model in ref. [19]. The results are derived from 10^4 realisations of the stochastic evolution.

conclusions apply to any model where the inflaton field crosses a plateau with an inflection point in order to generate a spike in the power spectrum and give rise to PBHs.

We expect therefore that the standard (classical) picture to evaluate the dark matter abundance in terms of PBHs is significantly altered.

7 Conclusions

There is a lot of interest in the cosmology community for the possibility that the dark matter is formed by PBHs. Their origin might be ascribed to the same mechanism giving rise to the CMB anisotropies and large-scale scale structure, i.e. a period of inflationary accelerated expansion during the early stages of evolution of the universe. In single-field models the power spectrum of the curvature perturbation might increase at small scales if the inflaton crosses a region which is flat enough and various models in the literature have been proposed recently.

In this paper we have discussed the role of quantum diffusion in the determination of the final abundance of PBHs. Quantum diffusion necessarily acquires importance when the force induced by the inflaton potential becomes tiny during the dynamics of the inflaton field. We have analysed both analytically and numerically the impact of diffusion and concluded that in realistic models it can significantly affect the capability of making a firm prediction of the PBH abundance. This is because the velocity of the inflaton field turns out to be distributed around its classical value with a spread which has an exponential impact on the PBH mass fraction.

While by itself the mass fraction does not say anything about the spatial distribution of the PBHs, we expect that different regions of the universe upon PBH formation would be populated with different relative abundances, thus changing the prediction for how much dark matter there is or its subsequent evolution.

JCAP07(2018)032

Acknowledgments

We thank M. Cicoli, F. G. Pedro, and G. Tasinato for many interactions about their work (refs. [18] and [19] respectively) and feedback on our draft. We also thank A. Linde for interactions about the PBH formation probability. A.R. is supported by the Swiss National Science Foundation (SNSF), project *Investigating the Nature of Dark Matter*, project number: 200020-159223. A.K. thanks the Cosmology group at the Département de Physique Théorique at the Université de Genève for the kind hospitality and financial support.

A The curvature perturbation, the Schwarzian derivative and the dual transformation

In this appendix we elaborate further the issue of why the power spectrum during the non-attractor phase is indeed flat. This appendix does not contain some new material with respect to the literature.

Our starting point is the equation for the curvature perturbation on comoving hypersurfaces $\mathcal{R}$

$$\mathcal{R}'' + 2\frac{z'}{z}\mathcal{R}' + k^2\mathcal{R} = 0, \tag{A.1}$$

where for convenience the prime denotes in this appendix and in the following one the conformal time derivative $\mathrm{d}/\mathrm{d}\tau$ and $z = a\dot{\phi}/H$ (the dot denotes the cosmic time derivative). The function z satisfies the following equation

$$\frac{z''}{z} = 2a^2H^2\left(1+\epsilon-\frac{3}{2}\eta+\epsilon^2-2\epsilon\eta+\frac{1}{2}\eta^2+\frac{1}{2}\xi^2\right) = 2a^2H^2\left(1+\frac{5}{2}\epsilon+\epsilon^2-2\epsilon\eta-\frac{1}{2}\frac{V_{,\phi\phi}}{H^2}\right), \tag{A.2}$$

where

$$\begin{aligned}\epsilon &= -\frac{\dot{H}}{H^2},\\ \eta &= -\frac{\ddot{\phi}}{H\dot{\phi}},\\ \xi^2 &= 3(\epsilon+\eta)-\eta^2-\frac{V_{,\phi\phi}}{H^2}.\end{aligned} \tag{A.3}$$

As long as slow-roll is attained, one can make use of the corresponding slow-roll parameters deduced from the form of the potential

$$\begin{aligned}\epsilon_V &= \frac{1}{2}\left(\frac{V_{,\phi}}{V}\right)^2,\\ \eta_V &= \frac{1}{3}\frac{V_{,\phi\phi}}{H^2},\\ \xi_V^2 &= 3\epsilon_V-\eta_V^2,\end{aligned} \tag{A.4}$$

where the dynamics around Hubble crossing is dominated by the exponentially growing friction term proportional to $\mathcal{R}'$, and the solution to eq. (A.1) is well approximated by

$$\mathcal{R}(\tau) = \text{constant} \quad \text{and} \quad \frac{\mathcal{R}'(\tau)}{aH} \sim \left(\frac{\tau}{\tau_k}\right)^2, \tag{A.5}$$

JCAP07(2018)032

where τ_k indicates the value of the conformal time at which the comoving wavelength $\sim 1/k$ leaves the comoving Hubble radius.

In the case in which one is interested in the generation of PBH from sizeable curvature fluctuations at small scales, a violent departure from the slow-roll must occur. In particular, if after Hubble crossing the friction term proportional to z'/z changes its sign from positive to negative, it may become a driving term. This can have significant effects on modes which leave or have left the Hubble radius during this transient and non-attractor epoch and thus induce a growth of the curvature perturbations [57, 58]. A necessary, but not sufficient condition, to have PBH generation from single-field models is therefore the presence of a transient period for which

$$\frac{z'}{z} = aH\,(1+\epsilon-\eta) < 0. \tag{A.6}$$

During such stage the function z reaches a local extremum (a maximum or a minimum depending upon the sign of $\dot{\phi}$) at some time whenever

$$1+\epsilon-\eta = 0, \tag{A.7}$$

Since ϵ is always positive, the presence of a transient stage implies that η must be at least unity, signalling a breakdown of the slow-roll conditions.

In order to simplify the problem of dealing with a non-attractor phase necessary to generate a large amount of PBHs, we start by noticing that, upon the redefinition

$$\mathcal{R} = \frac{\widetilde{z}}{z}\widetilde{\mathcal{R}}, \tag{A.8}$$

the quantity $\widetilde{\mathcal{R}}$ satisfies the same equation of $\mathcal{R}$

$$\widetilde{\mathcal{R}}'' + 2\frac{\widetilde{z}'}{\widetilde{z}}\widetilde{\mathcal{R}}' + k^2\widetilde{\mathcal{R}} = 0, \tag{A.9}$$

as long as

$$\frac{z''}{z} = \frac{\widetilde{z}''}{\widetilde{z}}. \tag{A.10}$$

The transformation from z to $\widetilde{z}$ which satisfies the relation (A.10) has been nicely worked out in ref. [55] and called a dual transformation. It reads

$$\widetilde{z}(\tau) = C_1 z(\tau) + C_2 z(\tau)\int^{\tau}\frac{\mathrm{d}\tau'}{z^2(\tau')}. \tag{A.11}$$

In fact this transformation is a property inferred from the so-called Schwarzian derivative [60], which we briefly summarise in the next subsection

The Schwarzian derivative. Given a function $f(\tau)$, the Schwarzian derivative is defined as

$$f \mapsto S[f] = \frac{f'''}{f'} - \frac{3}{2}\left(\frac{f''}{f'}\right)^2. \tag{A.12}$$

A property of the Schwarzian is that it is invariant under the transformation

$$\widetilde{f} = \frac{a\,f+b}{c\,f+d}, \qquad ad-bc \neq 0, \tag{A.13}$$

JCAP07(2018)032

that is

$$S[\widetilde{f}] = S[f]. \tag{A.14}$$

Note that the symmetry (A.14) is just $\mathrm{SL}(2,\mathbb{R})$ up to a rescaling of f. Consider now a differential equation

$$u'' + q(\tau)u = 0. \tag{A.15}$$

It can easily be seen that

$$q(\tau) = \frac{1}{2}S[f], \tag{A.16}$$

where

$$f(\tau) = \int^{\tau} \frac{\mathrm{d}\tau'}{u^2(\tau')}. \tag{A.17}$$

Indeed, from eq. (A.17) we find that

$$u = \frac{1}{\sqrt{f'}}, \tag{A.18}$$

and therefore,

$$u'' = -\frac{1}{2}S[f]u, \tag{A.19}$$

which is nothing else than eq. (A.15) and eq. (A.16). Now, since the Schwarzian is invariant under the transformation (A.13), we have that

$$\frac{u''}{u} = -\frac{1}{2}S[f] = -\frac{1}{2}S[\widetilde{f}] = \frac{\widetilde{u}''}{\widetilde{u}}, \tag{A.20}$$

where

$$\widetilde{u} = \frac{1}{\sqrt{\widetilde{f}'}}. \tag{A.21}$$

Then, using eqs. (A.13), (A.18) and (A.21) we find that

$$\widetilde{u} = u(C1 + C_2 f), \qquad C_1 = \frac{d}{\sqrt{ad-bc}}, \quad C_2 = \frac{c}{\sqrt{ad-bc}}, \tag{A.22}$$

which, by using eq. (A.17), is written as

$$\widetilde{u}(\tau) = C_1 u(\tau) + C_2 u(\tau) \int^{\tau} \frac{\mathrm{d}\tau'}{u^2(\tau)}, \tag{A.23}$$

which is nothing else than the dual transformation found in ref. [55].

Going back to the transformation (A.11), the power spectrum of the comoving curvature perturbation at the end of inflation reads

$$\mathcal{P}_{\mathcal{R}}\Big|_{\text{end of inflation}} = \frac{\widetilde{z}}{z}\mathcal{P}_{\widetilde{\mathcal{R}}}\Big|_{\text{end of inflation}}, \tag{A.24}$$

JCAP07(2018)032

from which we deduce that the power spectrum of the comoving curvature perturbation $\mathcal{R}$ is flat, a property that is inherited by the power spectrum of $\widetilde{\mathcal{R}}$ for which the dynamics is of the slow-roll nature. The question now is what is the most suitable dual transformation to perform in order to simplify the computation of the power spectrum for those modes which exit the Hubble radius during the non-attractor phase and which are ultimately responsible for the production of PBHs when these curvature perturbations re-enter the Hubble radius during the radiation phase.

As we have mentioned already several times, the production of PBHs may originated from the enhancement of the curvature power spectrum below a certain length scale. This can be achieved by a temporary abandonment of the slow-roll condition. When the inflaton field follows slow-roll and $\dot{\phi}$ is approximately constant, the function $z = a\dot{\phi}/H$ grows

$$z \sim \frac{1}{\tau} \quad \text{during slow-roll.} \tag{A.25}$$

During the non-attractor phase, when the inflaton field experiences an approximately flat potential and $V_{,\phi}$ can be neglected, it satisfies the equation of motion

$$\phi'' + 2\mathcal{H}\phi' \simeq 0 \quad (\mathcal{H} = aH), \tag{A.26}$$

and consequently $\phi' \sim \tau^2$, or

$$z = \frac{a\dot{\phi}}{H} = \frac{\phi'}{H} \sim \tau^2 \quad \text{during the non-attractor phase.} \tag{A.27}$$

It is this rapid fall of z which allows the possibility of enhancing the power spectrum. When the non-attractor phase is over, the slow-roll conditions are attained again and one recovers the behaviour in eq. (A.25). In terms of the friction term z'/z one has

$$\frac{z'}{z} \simeq aH \begin{cases} 1 & \text{during slow-roll,} \\ -2 & \text{during the non-attractor phase.} \end{cases} \tag{A.28}$$

Let us now use the dual transformation (A.11) where we choose the lower limit of the integral to be τ_0, the initial conformal time for the non-attractor phase. In such a case, we find

$$\frac{\widetilde{z}'}{\widetilde{z}} = \frac{z'}{z} + \frac{C_2}{z}\frac{1}{C_1 z + C_2 z\int_{\tau_0}^{\tau} \mathrm{d}\tau'/z^2(\tau')}. \tag{A.29}$$

We can now choose $C_1 = 1$ and compute this expression during the non-attractor phase for those modes which enter the Hubble radius during the non-attractor phase

$$\frac{1}{aH}\frac{\widetilde{z}'}{\widetilde{z}} = -2 + \frac{C_2}{aHz}\cdot\frac{1}{z + C_2 z\int_{\tau_0}^{\tau} \mathrm{d}\tau'/z^2(\tau')}. \tag{A.30}$$

Setting $a = a_0(\tau_0/\tau)$ and $z(\tau) = z_0(\tau/\tau_0)^2$, we obtain

$$\frac{1}{aH}\frac{\widetilde{z}'}{\widetilde{z}} = -2 + \frac{C_2}{a_0 z_0 H}\left(\frac{\tau_0}{\tau}\right)\frac{1}{z_0(\tau/\tau_0)^2 - (C_2/3z_0)(\tau_0^2/\tau)}. \tag{A.31}$$

where in the last passage we have neglected the subleading term $\sim 1/\tau_0^3$. Taking $-\tau < -\tau_0$ (recall that $\tau < 0$) and recalling that $a_0 = -1/(H\tau_0)$, one finally obtains

$$\frac{1}{aH}\frac{\widetilde{z}'}{\widetilde{z}} \simeq -2 + 3 = 1 \quad \text{(during the non-attractor phase).} \tag{A.32}$$

JCAP07(2018)032

This demonstrates that the choice

$$\widetilde{z}(\tau) = z(\tau) + C_2 z(\tau) \int_{\tau_0}^{\tau} \frac{\mathrm{d}\tau'}{z^2(\tau')}, \tag{A.33}$$

maps the non-attractor phase into a slow-roll phase for the curvature perturbation $\widetilde{\mathcal{R}}$ and one can conclude that the power spectrum of the curvature perturbation for those modes entering the Hubble radius during the non-attractor phase is dictated by a slow-roll dynamics and therefore is flat. Its amplitude is however magnified by a factor $\widetilde{z}(\tau_{\rm e})/z(\tau_{\rm e})$.

To elaborate further and find a useful prescription, let us consider, as we also did in the main text, Starobinsky's model [59] where the inflaton field reaches a non-attractor phase after a slow-roll era (and eventually enters afterwards another slow-roll phase).

Slow-roll phase before the non-attractor phase. If we indicate by ϕ_0 the moment at which the first slow-roll phase ends and the non-attractor phase starts, we can Taylor expand the inflaton potential as

$$V(\phi) \simeq V_0 \left(1 + \sqrt{2\epsilon_+}(\phi - \phi_0)\right) + \cdots \quad \text{for} \quad \phi > \phi_0, \tag{A.34}$$

where ϵ_+ is the slow-roll parameter during the first slow-roll phase. The corresponding parameter z reads

$$3\mathcal{H}\phi' = -V_{,\phi} a^2 \quad \text{and} \quad z_+(\tau) \simeq -a_0\sqrt{2\epsilon_+}(\tau_0/\tau), \tag{A.35}$$

having indicated τ_0 and a_0 is the conformal time and the scale factor when $\phi = \phi_0$, respectively.

Non-attractor phase. For $\phi < \phi_0$ the potential is Taylor expanded as

$$V(\phi) \simeq V_0 \left(1 + \sqrt{2\epsilon_-}(\phi - \phi_0)\right) + \cdots \quad \text{for} \quad \phi < \phi_0. \tag{A.36}$$

The dynamics leads to

$$\frac{3\mathcal{H}\phi'}{V_0 a^2} = -\sqrt{2\epsilon_-} - (\sqrt{2\epsilon_+} - \sqrt{2\epsilon_-})(\tau/\tau_0)^3 \tag{A.37}$$

and

$$z_-(\tau) \simeq -a_0 \left(\sqrt{2\epsilon_-}(\tau_0/\tau) + (\sqrt{2\epsilon_+} - \sqrt{2\epsilon_-})(\tau/\tau_0)^2\right). \tag{A.38}$$

If $\epsilon_+ \gg \epsilon_-$, there is a prolonged non-attractor phase where the second term in the above equation dominates over the first one. It is easy to show that z_- reaches a maximum at the point

$$(\tau_0/\tau_{\rm m})^3 = 2\frac{\sqrt{2\epsilon_+} - \sqrt{2\epsilon_-}}{\sqrt{2\epsilon_-}} \simeq 2\sqrt{\frac{\epsilon_+}{\epsilon_-}}, \tag{A.39}$$

corresponding to $z_-(\tau_{\rm m}) \approx (\epsilon_-/\epsilon_+)^{1/3} z(\tau_0)$ and causing a sizeable change in $\mathcal{R}$ on super-Hubble scales if $z_-(\tau_{\rm m})$ is very tiny. Notice that the smallness of ϵ_- parametrises the duration of the non-attractor phase from τ_0 to $\tau_\star$. Let us now consider the duality transformation (A.11) with again lower limit τ_0 in the integral. We deduce

$$\widetilde{z}_-(\tau) = -C_1 a_0 \sqrt{2\epsilon_-}(\tau_0/\tau) + \frac{a_0^3\sqrt{2\epsilon_-}(\sqrt{2\epsilon_-} - \sqrt{2\epsilon_+})C_1 + 3C_2 H^3}{a_0^2\sqrt{2\epsilon_-}}(\tau/\tau_0)^2. \tag{A.40}$$

JCAP07(2018)032

We are free to choose C_2 such that the second term on the right-hand side of eq. (A.40) vanishes, which happens for

$$C_2 = \frac{a_0^3\sqrt{2\epsilon_-}(\sqrt{2\epsilon_+} - \sqrt{2\epsilon_-})}{3H^3}\, C_1, \tag{A.41}$$

and hence

$$\widetilde{z}_-(\tau) = -C_1 a_0 \sqrt{2\epsilon_-}(\tau_0/\tau). \tag{A.42}$$

We are also free to make the dual transformation only for $\phi < \phi_0$ and therefore we match z_+ with the new $\widetilde{z}_-$ at τ_0 and find

$$C_1 = \sqrt{\frac{\epsilon_+}{\epsilon_-}}. \tag{A.43}$$

Therefore we have a single slow-roll parameter

$$z = z_+ = \widetilde{z}_- = -a_0\sqrt{2\epsilon_+}(\tau_0/\tau), \tag{A.44}$$

throughout all the evolution. This implies that the power spectrum for the $\widetilde{\mathcal{R}}$ not only remains constant after Hubble crossing, but also can be computed using the slow-roll approximations and it reads

$$\mathcal{P}_{\widetilde{\mathcal{R}}}^{1/2} = \left.\frac{3H^3}{2\pi V_0\sqrt{2\epsilon_+}}\right|_{k=aH}, \tag{A.45}$$

even during the non-attractor phase. The power spectrum therefore evolves as

$$\mathcal{P}_{\mathcal{R}}^{1/2}(\tau) = \frac{\widetilde{z}(\tau)}{z(\tau)}\mathcal{P}_{\widetilde{\mathcal{R}}}^{1/2} = \frac{\widetilde{z}_-(\tau)}{z_-(\tau)}\mathcal{P}_{\widetilde{\mathcal{R}}}^{1/2} = \frac{1}{\sqrt{2\epsilon_-/2\epsilon_+} + (1 - \sqrt{2\epsilon_-/2\epsilon_+})(\tau/\tau_0)^3}\mathcal{P}_{\widetilde{\mathcal{R}}}^{1/2}, \tag{A.46}$$

Defining by $\tau_\star$ the end of the non-attractor phase and computing the power spectrum just after $\tau_\star$ (recall that the conformal time is negative and therefore $-\tau_\star \ll -\tau_0$)) we find that immediately after the non-attractor phase

$$\mathcal{P}_{\mathcal{R}}^{1/2}(\tau \gtrsim \tau_\star) = \frac{\sqrt{2\epsilon_+}}{\sqrt{2\epsilon_-}}\mathcal{P}_{\widetilde{\mathcal{R}}}^{1/2} = \frac{3H^3}{2\pi V_0\sqrt{2\epsilon_-}}. \tag{A.47}$$

At the end of the non-attractor phase therefore one finds

$$\mathcal{P}_{\mathcal{R}}^{1/2}(\tau \gtrsim \tau_\star) = \left(\frac{H}{2\pi\Pi_\star}\right) = \left.\frac{3H^3}{2\pi V_{,\phi}}\right|_{k=aH}, \tag{A.48}$$

which provides the prescription to compute the power spectrum of the curvature perturbations for those modes crossing the Hubble radius deep in the non-attractor phase. By tuning the slope of the potential one can in principle obtain a large enhancement of the power spectrum.

A few comments are in order. The last passage in eq. (A.48) is valid only if the subsequent slow-roll phase starts when the velocity of the inflaton field has already settled to its slow-roll value proportional to $\sqrt{2\epsilon_-}$. We remind the reader that the power spectrum does not further evolve during the subsequent transition between the non-attractor phase

JCAP07(2018)032

and the second slow-roll phase [39]. The prescription (A.48) was already proposed in ref. [56] (see also refs. [55, 57, 58]) to deal with the singular case in which $\dot{\phi} = 0$. In this sense the results of this long appendix are not new, but we have given an alternative and maybe more intuitive derivation. Furthermore, the prescription (A.48) can be used for those modes which exit the Hubble radius deep in the non-attractor phase and predicts a flat power spectrum as the dual $\widetilde{R}$ experiences a slow-roll dynamics. Said in other words, the power spectrum must be flat since $\widetilde{z}''/\widetilde{z} = z''/z \simeq 2a^2H^2$ up to small correction $\mathcal{O}(\epsilon_V)$. If one wishes to compute the abundance of PBHs using single-field models where a non-attractor phase is necessary, the corresponding power spectrum of the comoving curvature perturbation can be computed by simply evaluating it at Hubble crossing, even during the non-attractor phase, as long as one makes use of the slow-roll relation $\dot{\phi} = -V_{,\phi}/3H$; one can then account for the modes leaving the Hubble radius when η grows fast from tiny values to 3 using eq. (2.8). Finally, the prescription is based on the fact that the non-attractor phase is long enough for the dynamics to established. If the plateau is short in field space, the inflaton field may arrive at it with an excessive kinetic energy and roll away of it in a Hubble time or so.

B From the non-attractor back to the slow-roll phase

The modes which have crossed the Hubble radius during the non-attractor phase are on super-Hubble scales during the eventual subsequent transition to a slow-roll phase with larger slope in the potential. To see what happens to these modes we follow ref. [39] and model again the potential during the transition as

$$V(\phi) \simeq V_0 \left(1 + \sqrt{2\epsilon_\star}(\phi - \phi_\star)\right) + \cdots , \tag{B.1}$$

where we have defined $\phi_\star$ the field value at the end of the attractor phase. The equation of motion for the inflaton field during the transition epoch reads

$$\phi'' + 3\mathcal{H}\phi' + 3a^2\sqrt{2\epsilon_\star} = 0, \tag{B.2}$$

whose solution for initial velocity $\Pi_\star$ leads to

$$z(\tau) = -\frac{\Pi_\star}{18}\left(3(6+h)(\tau/\tau_\star)^2 - 3h\frac{\tau_\star}{\tau}\right), \quad h = 6\sqrt{2\epsilon_\star}/\Pi_\star. \tag{B.3}$$

The solution for the super-Hubble scale comoving perturbation during the transient epoch reads

$$\mathcal{R}(\tau) = C_1 + C_2\int^\tau \frac{\mathrm{d}\tau}{z^2(\tau')} = C_1 + C_2\frac{12\tau_\star}{2(6+h)\epsilon_-(-h+(6+h)\tau^3)}. \tag{B.4}$$

This solution needs to be matched now with the solution for $\tau < \tau_\star$ which (apart from the standard $(H/2\pi)(1/\sqrt{2k^3})$ scales like $(\tau_\star/\tau)^3/\Pi_\star$. Matching the perturbations and their derivatives at $\tau_\star$, one gets

$$\mathcal{R}|_{\text{end of inflation}} = \left(\frac{H}{2\pi\sqrt{2k^3}}\right)\frac{6+h}{h\Pi_\star}. \tag{B.5}$$

We see that if the non-attractor phase is followed by another slow-roll phase for which $|h| \gg 1$, the curvature perturbations associated to the modes which are on super-Hubble scales during the transition will keep be enhanced as $1/\sqrt{2\epsilon_-}$ and the prescription (A.48) remains valid for those modes exiting the Hubble radius deep in the non-attractor phase [39].

JCAP07(2018)032

C The role of non-Gaussianities

As we mentioned in the introduction, PBHs are born as large, but rare fluctuations of the curvature perturbation. As such, their abundance is extremely sensitive to the non-linearities of the curvature perturbation. A formalism particularly useful when dealing with non-linearities is the so-called δN formalism [51], where the scalar field fluctuations are quantized on the flat slices and $\mathcal{R} = -\delta N$, being N the number of e-folds. The formalism is based on the assumption that on super-Hubble scales, each spatial point of the universe has an independent evolution and the latter is well approximated by the evolution of an unperturbed universe.

Let us suppose that during the entire non-attractor phase the inflaton velocity decays exponentially. If so

$$\mathcal{N}(\phi, \Pi) = -\frac{1}{3}\ln\left[\frac{\Pi}{\Pi + 3H(\phi - \phi_\star)}\right] = -\frac{1}{3}\ln\frac{\Pi}{\Pi_\star}, \tag{C.1}$$

where $\phi_\star$ is again the value of the field at the end of the non-attractor phase. Notice that we have retained the dependence on Π since slow-roll is badly violated. In the relation (C.1) we have followed the notation of ref. [39] and defined $\mathcal{N} = 0$ to be the end of the attractor phase, so that $\mathcal{N} < 0$ and

$$\phi(\mathcal{N}) = \phi_\star + \frac{\Pi_\star}{3}\left(1 - e^{-3\mathcal{N}}\right) \quad \text{and} \quad \Pi(\mathcal{N}) = \Pi_\star e^{-3\mathcal{N}}. \tag{C.2}$$

We therefore find that

$$\mathcal{R} = -\delta\mathcal{N} = -\mathcal{N} + \overline{\mathcal{N}} = -\frac{1}{3}\ln\left(1 + \frac{\delta\Pi_\star}{\overline{\Pi}_\star}\right), \tag{C.3}$$

where the overlines indicate the corresponding background values. One can safely neglect the perturbation $\delta\Pi$ as it decays exponentially fast. On the other hand, by using the relation

$$\Pi_\star = 3\left[\phi(\mathcal{N}) - \phi_\star\right] + \Pi(\mathcal{N}), \tag{C.4}$$

we see that up to irrelevant constants,

$$\mathcal{R} = -\frac{1}{3}\ln\left(1 + 3\frac{\delta\phi}{\overline{\Pi}_\star}\right), \quad \delta\phi < -\frac{\Pi_\star}{3}. \tag{C.5}$$

The crucial point now is that the dynamics of $\delta\phi$ is the one of a massless perturbation in de Sitter and to a very good approximation its behaviour is Gaussian. The non-Gaussianity in the curvature perturbation arises because of the non-linear mapping between $\delta\phi$ and $\mathcal{R}$.[1]

[1] A few comments. The non-Gaussianity during the non-attractor phase is not washed out by the subsequent transition to a slow-roll phase. This is because such a transition is sudden [39] as the velocity during the non-attractor phase must be much smaller than the one during the subsequent slow-roll phase to generate PBHs. The non-Gaussianity we are dealing with here is not the non-Gaussianity in the squeezed configuration which peaks when one of the wavelengths is much larger than the other two. This non-Gaussianity is not observable by a local observer testing a region much smaller than the long wavelength [63]. We are instead referring to that non-Gaussianity which arises at the same small wavelengths where the density perturbations are sizeable. In the limit of a spiked power spectrum centered around a given momentum $k_{\rm pk}$, the non-Gaussianity will be peaked at equilateral configurations.

JCAP07(2018)032

The fact that $P(\delta\phi)$ is Gaussian considerably simplifies the computation: the primordial mass fraction $\beta_{\rm prim}(M)$ of the universe occupied by PBHs at formation time is dictated by probability conservation,

$$P(\mathcal{R}) = \left|\frac{\mathrm{d}\delta\phi}{\mathrm{d}\mathcal{R}}\right| P[\delta\phi(\mathcal{R})], \tag{C.6}$$

or

$$P(\mathcal{R}) = \frac{|\overline{\Pi}_\star|}{\sqrt{2\pi}\,\sigma_{\delta\phi}} \exp\left[-3\mathcal{R} - \frac{\overline{\Pi}_\star^2}{18\sigma_{\delta\phi}^2}\left(1-e^{-3\mathcal{R}}\right)^2\right], \tag{C.7}$$

where we have written the Gaussian distribution of $\delta\phi$ as[2]

$$P(\delta\phi) = \frac{1}{\sqrt{2\pi}\,\sigma_{\delta\phi}} e^{-(\delta\phi)^2/2\sigma_{\delta\phi}^2}, \tag{C.8}$$

with

$$\sigma_{\delta\phi}^2 = \int_k \mathrm{d}\ln p\, \mathcal{P}_{\delta\phi}(p). \tag{C.9}$$

For $3\mathcal{R}_c \lesssim 1$, we obtain

$$P(\mathcal{R}) \approx \frac{\overline{\Pi}_\star}{\sqrt{2\pi}\,\sigma_{\delta\phi}} e^{-\overline{\Pi}_\star^2\mathcal{R}^2/2\sigma_{\delta\phi}^2}, \tag{C.10}$$

i.e., a Gaussian with variance

$$\sigma_{\mathcal{R}}^2 = \frac{\sigma_{\delta\phi}^2}{\overline{\Pi}_\star^2}. \tag{C.11}$$

On the other hand, assuming now $3\mathcal{R}_c \gtrsim 1$, we obtain

$$\begin{aligned}\beta_{\rm prim}(M) &= \int_{\mathcal{R}_c} \mathrm{d}\mathcal{R}\, P(\mathcal{R}) \simeq \frac{1}{2}\mathrm{erf}\left(\frac{\overline{\Pi}_\star}{3\sqrt{2}\sigma_{\delta\phi}}\right) - \frac{1}{2}\mathrm{erf}\left(\frac{\overline{\Pi}_\star(1-e^{-3\mathcal{R}_c})}{3\sqrt{2}\sigma_{\delta\phi}}\right)\\ &\simeq -\frac{\Pi_\star e^{-3\mathcal{R}_c}}{3\sqrt{2\pi}\,\sigma_{\delta\phi}} e^{-\Pi_\star^2/18\sigma_{\delta\phi}^2},\end{aligned} \tag{C.12}$$

to be confronted to the Gaussian result (6.9). The probability is clearly non- Gaussian. We can estimate $\sigma_{\delta\phi}$ as well to be of the order of $(H/2\pi)\Delta N$. We obtain

$$\beta_{\rm prim}(M) \simeq \frac{e^{-3\mathcal{R}_c}}{3\mathcal{R}_\star\Delta N} e^{-1/(3\sqrt{2}\mathcal{R}_\star\Delta N)^2}. \tag{C.13}$$

To obtain the same primordial mass fraction, non-Gaussianity seems to require a smaller $\mathcal{R}_\star$. We write "seems" as the curvature perturbation is not the best variable to study the PBH mass function. As written in the main text, the density contrast $\Delta(\vec{x}) = (4/9a^2H^2)\nabla^2\zeta(\vec{x})$ (during radiation) is the good variable [26]. This however will make things more difficult to analyse because of the complication arising from taking the laplacian of the expression (C.3). One possible, but not entirely satisfactory, way out might to evaluate the density contrast at Hubble re-entry, i.e. setting $k = aH$. In such a case, one could relate the density contrast to the curvature perturbation through the relation $\Delta(\vec{x}) = (4/9)\mathcal{R}(\vec{x})$.

[2]Sometimes the Gaussian probability is multiplied by a factor of 2 to account for the fact that one deals with a first time-passage problem [62]. We do not put it here as there is no general consensus of this factor. Quantitatively, it does not make a big difference though.

JCAP07(2018)032

References

[1] B.J. Carr and S.W. Hawking, *Black holes in the early Universe*, *Mon. Not. Roy. Astron. Soc.* **168** (1974) 399 [INSPIRE].

[2] P. Meszaros, *The behaviour of point masses in an expanding cosmological substratum*, *Astron. Astrophys.* **37** (1974) 225 [INSPIRE].

[3] B.J. Carr, *The Primordial black hole mass spectrum*, *Astrophys. J.* **201** (1975) 1 [INSPIRE].

[4] S. Bird et al., *Did LIGO detect dark matter?*, *Phys. Rev. Lett.* **116** (2016) 201301 [arXiv:1603.00464] [INSPIRE].

[5] S. Clesse and J. García-Bellido, *The clustering of massive Primordial Black Holes as Dark Matter: measuring their mass distribution with Advanced LIGO*, *Phys. Dark Univ.* **15** (2017) 142 [arXiv:1603.05234] [INSPIRE].

[6] M. Sasaki, T. Suyama, T. Tanaka and S. Yokoyama, *Primordial Black Hole Scenario for the Gravitational-Wave Event GW150914*, *Phys. Rev. Lett.* **117** (2016) 061101 [arXiv:1603.08338] [INSPIRE].

[7] M. Sasaki, T. Suyama, T. Tanaka and S. Yokoyama, *Primordial black holes — perspectives in gravitational wave astronomy*, *Class. Quant. Grav.* **35** (2018) 063001 [arXiv:1801.05235] [INSPIRE].

[8] B. Carr, M. Raidal, T. Tenkanen, V. Vaskonen and H. Veermäe, *Primordial black hole constraints for extended mass functions*, *Phys. Rev.* **D 96** (2017) 023514 [arXiv:1705.05567] [INSPIRE].

[9] M. Zumalacarregui and U. Seljak, *No LIGO MACHO: Primordial Black Holes, Dark Matter and Gravitational Lensing of Type Ia Supernovae*, arXiv:1712.02240 [INSPIRE].

[10] J. García-Bellido, S. Clesse and P. Fleury, *Primordial black holes survive SN lensing constraints*, *Phys. Dark Univ.* **20** (2018) 95 [arXiv:1712.06574] [INSPIRE].

[11] Virgo, LIGO Scientific collaboration, B.P. Abbott et al., *Observation of Gravitational Waves from a Binary Black Hole Merger*, *Phys. Rev. Lett.* **116** (2016) 061102 [arXiv:1602.03837] [INSPIRE].

[12] P. Ivanov, P. Naselsky and I. Novikov, *Inflation and primordial black holes as dark matter*, *Phys. Rev.* **D 50** (1994) 7173 [INSPIRE].

[13] J. García-Bellido, A.D. Linde and D. Wands, *Density perturbations and black hole formation in hybrid inflation*, *Phys. Rev.* **D 54** (1996) 6040 [astro-ph/9605094] [INSPIRE].

[14] P. Ivanov, *Nonlinear metric perturbations and production of primordial black holes*, *Phys. Rev.* **D 57** (1998) 7145 [astro-ph/9708224] [INSPIRE].

[15] J. García-Bellido and E. Ruiz Morales, *Primordial black holes from single field models of inflation*, *Phys. Dark Univ.* **18** (2017) 47 [arXiv:1702.03901] [INSPIRE].

[16] K. Kannike, L. Marzola, M. Raidal and H. Veermäe, *Single Field Double Inflation and Primordial Black Holes*, *JCAP* **09** (2017) 020 [arXiv:1705.06225] [INSPIRE].

[17] G. Ballesteros and M. Taoso, *Primordial black hole dark matter from single field inflation*, *Phys. Rev.* **D 97** (2018) 023501 [arXiv:1709.05565] [INSPIRE].

[18] M. Cicoli, V.A. Diaz and F.G. Pedro, *Primordial Black Holes from String Inflation*, *JCAP* **06** (2018) 034 [arXiv:1803.02837] [INSPIRE].

[19] O. Özsoy, S. Parameswaran, G. Tasinato and I. Zavala, *Mechanisms for Primordial Black Hole Production in String Theory*, *JCAP* **07** (2018) 005 [arXiv:1803.07626] [INSPIRE].

[20] M. Kawasaki, N. Kitajima and T.T. Yanagida, *Primordial black hole formation from an axionlike curvaton model*, *Phys. Rev.* **D 87** (2013) 063519 [arXiv:1207.2550] [INSPIRE].

JCAP07(2018)032

[21] B. Carr, F. Kuhnel and M. Sandstad, *Primordial Black Holes as Dark Matter*, *Phys. Rev.* **D 94** (2016) 083504 [arXiv:1607.06077] [INSPIRE].

[22] J. García-Bellido, M. Peloso and C. Unal, *Gravitational waves at interferometer scales and primordial black holes in axion inflation*, *JCAP* **12** (2016) 031 [arXiv:1610.03763] [INSPIRE].

[23] B. Carr, T. Tenkanen and V. Vaskonen, *Primordial black holes from inflaton and spectator field perturbations in a matter-dominated era*, *Phys. Rev.* **D 96** (2017) 063507 [arXiv:1706.03746] [INSPIRE].

[24] J.R. Espinosa, D. Racco and A. Riotto, *Cosmological Signature of the Standard Model Higgs Vacuum Instability: Primordial Black Holes as Dark Matter*, *Phys. Rev. Lett.* **120** (2018) 121301 [arXiv:1710.11196] [INSPIRE].

[25] T. Harada, C.-M. Yoo and K. Kohri, *Threshold of primordial black hole formation*, *Phys. Rev.* **D 88** (2013) 084051 [*Erratum ibid.* **89** (2014) 029903] [arXiv:1309.4201] [INSPIRE].

[26] S. Young, C.T. Byrnes and M. Sasaki, *Calculating the mass fraction of primordial black holes*, *JCAP* **07** (2014) 045 [arXiv:1405.7023] [INSPIRE].

[27] I. Musco and J.C. Miller, *Primordial black hole formation in the early universe: critical behaviour and self-similarity*, *Class. Quant. Grav.* **30** (2013) 145009 [arXiv:1201.2379] [INSPIRE].

[28] H. Motohashi and W. Hu, *Primordial Black Holes and Slow-Roll Violation*, *Phys. Rev.* **D 96** (2017) 063503 [arXiv:1706.06784] [INSPIRE].

[29] D.H. Lyth and A. Riotto, *Particle physics models of inflation and the cosmological density perturbation*, *Phys. Rept.* **314** (1999) 1 [hep-ph/9807278] [INSPIRE].

[30] W.H. Kinney, *Horizon crossing and inflation with large eta*, *Phys. Rev.* **D 72** (2005) 023515 [gr-qc/0503017] [INSPIRE].

[31] C. Dvorkin and W. Hu, *Generalized Slow Roll for Large Power Spectrum Features*, *Phys. Rev.* **D 81** (2010) 023518 [arXiv:0910.2237] [INSPIRE].

[32] M.H. Namjoo, H. Firouzjahi and M. Sasaki, *Violation of non-Gaussianity consistency relation in a single field inflationary model*, *EPL* **101** (2013) 39001 [arXiv:1210.3692] [INSPIRE].

[33] J. Martin, H. Motohashi and T. Suyama, *Ultra Slow-Roll Inflation and the non-Gaussianity Consistency Relation*, *Phys. Rev.* **D 87** (2013) 023514 [arXiv:1211.0083] [INSPIRE].

[34] X. Chen, H. Firouzjahi, M.H. Namjoo and M. Sasaki, *A Single Field Inflation Model with Large Local Non-Gaussianity*, *EPL* **102** (2013) 59001 [arXiv:1301.5699] [INSPIRE].

[35] S. Mooij and G.A. Palma, *Consistently violating the non-Gaussian consistency relation*, *JCAP* **11** (2015) 025 [arXiv:1502.03458] [INSPIRE].

[36] C. Germani and T. Prokopec, *On primordial black holes from an inflection point*, *Phys. Dark Univ.* **18** (2017) 6 [arXiv:1706.04226] [INSPIRE].

[37] K. Dimopoulos, *Ultra slow-roll inflation demystified*, *Phys. Lett.* **B 775** (2017) 262 [arXiv:1707.05644] [INSPIRE].

[38] B. Finelli, G. Goon, E. Pajer and L. Santoni, *Soft Theorems For Shift-Symmetric Cosmologies*, *Phys. Rev.* **D 97** (2018) 063531 [arXiv:1711.03737] [INSPIRE].

[39] Y.-F. Cai, X. Chen, M.H. Namjoo, M. Sasaki, D.-G. Wang and Z. Wang, *Revisiting non-Gaussianity from non-attractor inflation models*, *JCAP* **05** (2018) 012 [arXiv:1712.09998] [INSPIRE].

[40] J.M. Ezquiaga, J. García-Bellido and E. Ruiz Morales, *Primordial Black Hole production in Critical Higgs Inflation*, *Phys. Lett.* **B 776** (2018) 345 [arXiv:1705.04861] [INSPIRE].

JCAP07(2018)032

[41] S. Young and C.T. Byrnes, *Primordial black holes in non-Gaussian regimes*, *JCAP* **08** (2013) 052 [arXiv:1307.4995] [INSPIRE].

[42] E.V. Bugaev and P.A. Klimai, *Primordial black hole constraints for curvaton models with predicted large non-Gaussianity*, *Int. J. Mod. Phys.* **D 22** (2013) 1350034 [arXiv:1303.3146] [INSPIRE].

[43] J.S. Bullock and J.R. Primack, *NonGaussian fluctuations and primordial black holes from inflation*, *Phys. Rev.* **D 55** (1997) 7423 [astro-ph/9611106] [INSPIRE].

[44] J. Yokoyama, *Chaotic new inflation and formation of primordial black holes*, *Phys. Rev.* **D 58** (1998) 083510 [astro-ph/9802357] [INSPIRE].

[45] R. Saito, J. Yokoyama and R. Nagata, *Single-field inflation, anomalous enhancement of superhorizon fluctuations and non-Gaussianity in primordial black hole formation*, *JCAP* **06** (2008) 024 [arXiv:0804.3470] [INSPIRE].

[46] C.T. Byrnes, E.J. Copeland and A.M. Green, *Primordial black holes as a tool for constraining non-Gaussianity*, *Phys. Rev.* **D 86** (2012) 043512 [arXiv:1206.4188] [INSPIRE].

[47] S. Young, D. Regan and C.T. Byrnes, *Influence of large local and non-local bispectra on primordial black hole abundance*, *JCAP* **02** (2016) 029 [arXiv:1512.07224] [INSPIRE].

[48] M. Kawasaki and Y. Tada, *Can massive primordial black holes be produced in mild waterfall hybrid inflation?*, *JCAP* **08** (2016) 041 [arXiv:1512.03515] [INSPIRE].

[49] C. Pattison, V. Vennin, H. Assadullahi and D. Wands, *Quantum diffusion during inflation and primordial black holes*, *JCAP* **10** (2017) 046 [arXiv:1707.00537] [INSPIRE].

[50] G. Franciolini, A. Kehagias, S. Matarrese and A. Riotto, *Primordial Black Holes from Inflation and non-Gaussianity*, *JCAP* **03** (2018) 016 [arXiv:1801.09415] [INSPIRE].

[51] M. Sasaki and E.D. Stewart, *A General analytic formula for the spectral index of the density perturbations produced during inflation*, *Prog. Theor. Phys.* **95** (1996) 71 [astro-ph/9507001] [INSPIRE].

[52] A.D. Linde, *Particle physics and inflationary cosmology*, *Contemp. Concepts Phys.* **5** (1990) 1 [hep-th/0503203] [INSPIRE].

[53] H. Risken, *The Fokker-Planck equation*, Springer-Verlag, Berlin Germany (1984).

[54] R.F. Pawula, *Approximation of the Linear Boltzmann Equation by the Fokker-Planck Equation*, *Phys. Rev.* **D 162** (1967) 186.

[55] D. Wands, *Duality invariance of cosmological perturbation spectra*, *Phys. Rev.* **D 60** (1999) 023507 [gr-qc/9809062] [INSPIRE].

[56] O. Seto, J. Yokoyama and H. Kodama, *What happens when the inflaton stops during inflation*, *Phys. Rev.* **D 61** (2000) 103504 [astro-ph/9911119] [INSPIRE].

[57] S.M. Leach, M. Sasaki, D. Wands and A.R. Liddle, *Enhancement of superhorizon scale inflationary curvature perturbations*, *Phys. Rev.* **D 64** (2001) 023512 [astro-ph/0101406] [INSPIRE].

[58] S.M. Leach and A.R. Liddle, *Inflationary perturbations near horizon crossing*, *Phys. Rev.* **D 63** (2001) 043508 [astro-ph/0010082] [INSPIRE].

[59] A.A. Starobinsky, *Spectrum of adiabatic perturbations in the universe when there are singularities in the inflation potential*, *JETP Lett.* **55** (1992) 489 [INSPIRE].

[60] Z. Nehari, *Conformal mapping*, *Dover Books on Mathematics*, Dover Publications, Mineola U.S.A. (1952).

JCAP07(2018)032

[61] M. Sasaki and E.D. Stewart, *A General analytic formula for the spectral index of the density perturbations produced during inflation*, *Prog. Theor. Phys.* **95** (1996) 71 [astro-ph/9507001] [INSPIRE].

[62] M. Maggiore and A. Riotto, *The Halo Mass Function from Excursion Set Theory. I. Gaussian fluctuations with non-Markovian dependence on the smoothing scale*, *Astrophys. J.* **711** (2010) 907 [arXiv:0903.1249] [INSPIRE].

[63] R. Bravo, S. Mooij, G.A. Palma and B. Pradenas, *Vanishing of local non-Gaussianity in canonical single field inflation*, *JCAP* **05** (2018) 025 [arXiv:1711.05290] [INSPIRE].

JCAP07(2018)032